学位論文 (要約)

Study of cisternal maturation of the Golgi apparatus in *Saccharomyces cerevisiae*
(出芽酵母におけるゴルジ体槽成熟機構の研究)

平成 28 年 12 月 博士 (理学) 申請

東京大学大学院理学系研究科
生物科学専攻
石井　みどり

Abstract

Proteins synthesized in the endoplasmic reticulum (ER) are transported to the Golgi apparatus and then sorted to their destinations. For their passage through the Golgi apparatus, one widely accepted mechanism is cisternal maturation. Cisternal maturation is fulfilled by the retrograde transport of Golgi resident proteins from later to earlier cisternae, and candidate carriers for this retrograde transport are COPI-coated vesicles. I examined the COPI function in cisternal maturation directly by 4D observation of the transmembrane Golgi resident proteins in living yeast cells. COPI temperature-sensitive mutants and induced degradation of COPI proteins were used to knock down COPI function. By either way, inactivation of COPI subunits Ret1 and Sec21 markedly impaired the transition from *cis* to medial and to *trans* cisternae. Furthermore, the movement of cisternae within the cytoplasm was severely restricted when COPI subunits were depleted. These results demonstrate the essential roles of COPI proteins in retrograde trafficking of the Golgi resident proteins and dynamics of the Golgi cisternae.

To understand the selective sorting of vesicles between the Golgi cisterenae, I investigated the molecular arrangements of the conserved oligomeric Golgi (COG) subunits *in vivo*. I analyzed the endogenous protein interactions among COG subunits in cytosolic and membrane fractions by co-immunoprecipitation. Cytosolic COG subunits existed as octamers. Membrane-associated COG subunits form a variety of subcomplexes. Relocation of individual COG subunits to mitochondria resulted in recruitment of other subunits to mitochondria. I have shown *in vivo* interactions among COG subunits.

Contents

Acknowledgments

I would like to thank Professor Akihiko Nakano, Dr. Kazuo Kurokawa for advice and discussion throughout this study.

I would like to thank Professor Vladimir Lupashin of the University of Arkansas for Medical Sciences, U. S. A., for letting me visit and stay at his laboratory and conduct collaborative work on COG proteins.

I would like to thank all the members of the Nakano laboratory in The University of Tokyo and RIKEN Center for Advanced Photonics, especially Dr. Ryogo Hirata and Dr. Yasuyuki Suda for their help on yeast work, Dr. Masakazu Iwai for his help on protein work and Dr. Yoko Ito for her valuable comments and discussion.

I thank the Advanced Leading Graduate Course for Photon Science of The University of Tokyo for financial support to enable my research stay in the Lupashin laboratory.

Abbreviations

ER	endoplasmic reticulum
ERES	ER exit sites
CATCHR	complexes associated with tethering containing helical rods
COG complex	conserved oligomeric Golgi complex
COPI	coat protein complex I
CPY	carboxypeptidase Y
GFP	green fluorescent protein
mRFP	monomeric red fluorescent protein
NAA	1-naphthaleneacetic acid
SCLIM	super-resolution confocal live imaging microscopy
TGN	*trans*-Golgi network

General introduction

Eukaryotic cells have several intra-cellular membrane-bounded compartments called organelles. Each of them is a specific unit for the distinct functions in a cell. It is important for organelles to maintain the characteristic molecular compositions and traffic molecules between the other organelles to play their part. Protein and lipid transport between the organelles is mediated by membrane carriers, such as vesicles and tubules that bud from a donor membrane and fuse with a target membrane. The transport of these cargo molecules is highly regulated by many proteins including vesicle coat and tethering proteins. These membrane-bound transports are called membrane trafficking. The Golgi apparatus is a single-membrane-bounded organelle that works as a central station of the membrane trafficking system in eukaryotic cells. It consists of flattened membrane-enclosed compartments, called cisternae, which are orderly differentiated in their functions and structures from *cis* to *trans*. The Golgi apparatus receives newly synthesized proteins from the endoplasmic reticulum (ER) at *cis* cisternae, processes and glycosylates them as they proceed through the medial regions, and finally sorts them from *trans* cisternae and the *trans*-Golgi network (TGN) to their final destinations. Each cisterna has specific resident proteins. These functions of the Golgi apparatus are evolutionarily conserved. However, the organization of the Golgi apparatus varies across cell types and species; animal and plant cells have stacked Golgi cisternae, whereas the budding yeast *Saccharomyces cerevisiae* has unstacked cisternae dispersed in the cytoplasm (Mowbrey and Dacks 2009). Cisternae in a stacked Golgi is closely associated each other, which makes hard to observe single cisterna

under light microscopy. The unique feature of unstacked cisternae in *S. cerevisiae* is a powerful model system to observe protein trafficking between individual cisternae by live cell imaging.

The mechanism of protein trafficking within the Golgi apparatus is a fundamental and intriguing question of cell biology. For a long time, the Golgi cisternae are thought to be stable compartments that contain specific resident proteins. In this thought, secretory proteins move through the Golgi apparatus from *cis* cisternae to *trans* cisternae by anterograde transport vesicles whereas the Golgi resident proteins are stay in the cisternae (Rothman and Wieland 1996). This model is supported by some studies that identified vesicles around the Golgi apparatus contain several secretory cargos (Ostermann et al. 1993, Orci et al. 1997, Malsam et al. 2005, Pellett et al. 2013) (Fig. 1A). However this stable compartment model could not explain large aggregates of procollagen progressively moved through the Golgi stacks without leaving the lumen in mammalian cells (Bonfanti et al. 1998). To explain anterograde transport of secretory cargos including large aggregates, "cisternal maturation" model is now widely accepted as the core mechanism for Golgi traffic (Glick and Nakano 2009, Nakano and Luini 2010, Glick and Luini 2011). This model is based on the concept that Golgi cisternae progressively change their nature and work as anterograde carriers for secretory protein transport. The Golgi cisternae are transient compartments that carry secretory proteins anterograde direction and change their protein compositions by retrogradely recycling the resident proteins from *trans* to *cis* direction (Fig. 1B). The change of cisternal feature from *cis* to *trans* is called cisternal maturation. Maturation of the Golgi cisternae

has been directly observed in *S. cerevisiae* that has unstacked cisternae (Losev et al. 2006, Matsuura-Tokita et al. 2006). Individual early and late Golgi resident proteins were tagged with different fluorescent proteins to label early and late Golgi cisternae in *S. cerevisiae*. The colors of cisternae showed a unidirectional change from early to late under a confocal fluorescence microscope. In this view, Golgi resident proteins should be transported from late to early cisternae by retrograde transport mechanisms. Furthermore Rizzo et al. (2013) reported that artificial polymerization of Golgi resident proteins to prevent recycling led to their progression through the Golgi stack, which also supports cisternal maturation (Rizzo et al. 2013). However, many questions remain as to its molecular mechanisms.

Coat protein complex I (COPI)-coated vesicles are the candidate for retrograde transport carriers of Golgi resident proteins. COPI-coated vesicles bud off from the Golgi membrane. COPI coats are composed of seven subunits, known as α, β, β', γ, δ, ε and ζ COP, which are classified into two groups: α, β' and ε subunits forming the B trimeric adaptor complex, and β, γ, δ and ζ subunits forming the F tetrameric outer coat complex (Gabriely et al. 2007, Lee and Goldberg 2010). A function of COPI-coated vesicles in anterograde cargo transport is still a matter of debate, however COPI has pivotal roles in Golgi-ER retrograde transport and probably also in the retrograde traffic between Golgi cisternae (Orci et al. 2000, Martinez-Menarguez et al. 2001, Sato et al. 2001, Cosson et al. 2002, Rabouille and Klumperman 2005, Emr et al. 2009). In *S. cerevisiae*, Vps74 binds to the Golgi glycosylation enzymes to promote packing into the COPI-coated vesicles and maintains

their steady state distributions (Schmitz et al. 2008, Tu et al. 2008). Recruitment of COPI coat proteins to the Golgi membrane requires Arf GTPase (Serafini et al. 1991). A recent report has shown that disruption of Arf1 causes early Golgi cisternae to mature more slowly and less frequently but does not alter the maturation of late Golgi cisternae in *S. cerevisiae* (Bhave et al. 2014). These studies support intra-Golgi retrograde transport by COPI proteins, although the role of COPI-dependent traffic is not yet clear.

Conserved oligomeric Golgi (COG) complex is multi-subunit tethering complex of COPI-coated transport carriers at the target membrane. COG complex contains eight subunits (Cog1–8) and regulates early steps of the secretory pathway (Wuestehube et al. 1996, VanRheenen et al. 1998, VanRheenen et al. 1999). COG proteins localize at the Golgi cisternae and interact with proteins involving in the intra-Golgi trafficking. Vesicle tethering is the initial step for a transport carrier at its destination membrane before fusion of the membrane. How COPI-coated transport carriers are sorted and recognized at the target membrane is not fully understood.

In this doctoral study, I aimed at understanding the molecular mechanisms of cisternal maturation of the Golgi apparatus. I have focused on the analyses of COPI proteins and its tethering complex, the conserved oligomeric Golgi (COG) complex, at the Golgi membrane. For this aim, I took advantage of the live cell imaging of yeast Golgi apparatus. Live cell imaging is a very powerful and promising approach to many biological questions and gives us the spatial and temporal information of fluorescent-tagged proteins.

In Chapter 1, I will describe the detailed observation of the cisternal

maturation. To analyze the COPI function, COPI proteins were depleted by a temperature sensitive mutant and inducible degron system. In Chapter 2, I will describe interactions between the subunits of a COPI tethering complex, COG complex. COG subunits were analyzed by subcellular fractionation and co-immunoprecipitation. To further investigate the function of COG subunits, I conducted COG relocation assay and analyzed protein interactions were analyzed. Altogether, I have shown a part of mechanisms of intra-Golgi trafficking.

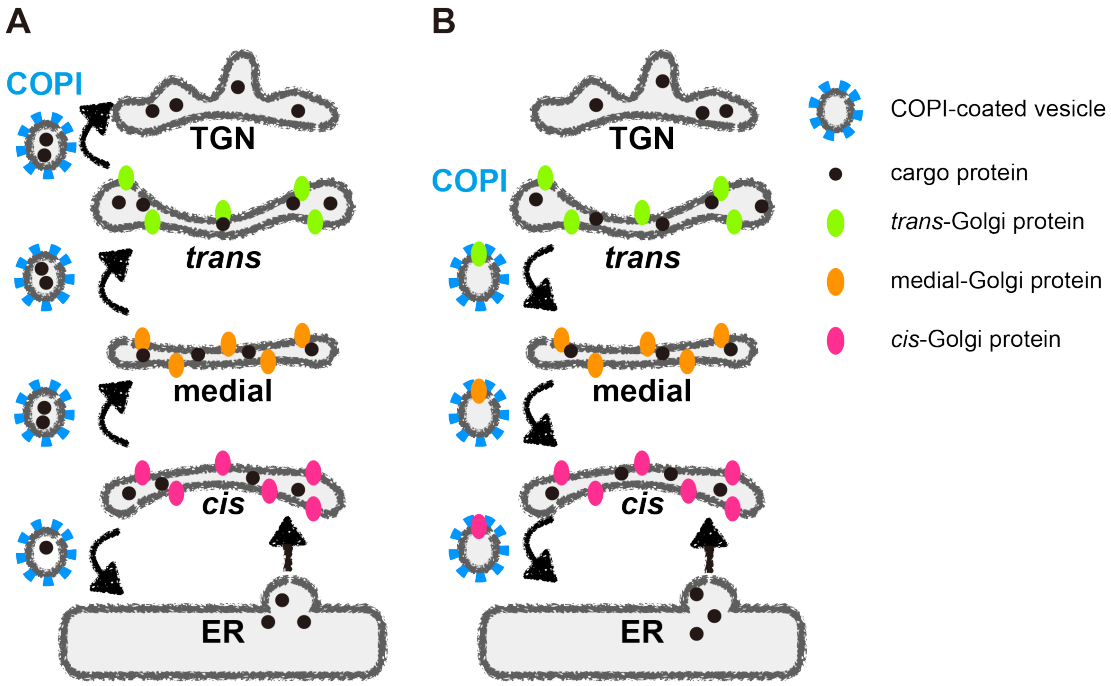

Figure 1 **Models for intra-Golgi trafficking.** (A) Stable compartment model. Anterograde COPI-coated vesicles transport cargo proteins from *cis* to *trans* direction. The Golgi resident proteins stay in the cisternae. (B) Cisternal maturation model. Cargo proteins remain in the cisternae. The Golgi resident proteins recycle back from later to earlier cisternae by retrograde COPI-coated vesicles.

Chapter 1.
Introduction

As described in the general introduction, COPI proteins are the candidate for retrograde transport carriers of Golgi resident proteins. In a previous report, α-COP temperature sensitive mutant, *ret1-1*, defective in COPI vesicle formation at the restrictive temperature, exhibited retarded but not completely blocked maturation from early to late cisternae at the restrictive temperature by 2D time-lapse observations (Matsuura-Tokita et al. 2006). From this result, the authors concluded that COPI is important for Golgi cisternal maturation, but other mechanisms might also operate. For technical reasons 3D observation was not performed, and they could not rule out the ambiguity of analysis from 2D data. To further clarify the role of COPI proteins in the cisternal maturation, I decided to revisit these issues by using transmembrane Golgi resident proteins as *cis-,* medial-, and *trans*-cisternal markers and by a more-elaborate 3D observation by high-speed and high-resolution confocal microscopy (super-resolution confocal live imaging microscopy, SCLIM) (Kurokawa et al. 2013). To inactivate COPI functions, not only temperature-sensitive defects of COPI proteins, but also a new method to induce their degradation by an auxin degron system (Nishimura et al. 2009) was employed. I found that disruption of COPI functions inhibited cisternal maturation and dynamic movement of cisternae in the cytoplasm. These results indicate that the retrograde transport of the Golgi-resident proteins is mediated through a COPI-dependent mechanism that plays a pivotal role in the cisternal maturation, and that COPI proteins also play other roles in the Golgi dynamics.

Results

Spatial distribution of transmembrane Golgi resident proteins

A variety of fluorescent-tagged proteins have been used for live imaging of yeast Golgi cisternae (Matsuura-Tokita et al. 2006). Here I employ Golgi resident proteins harboring transmembrane domains, which are Mnn9, a subunit of Golgi mannosyltransferase complex, Gnt1, an *N*-acetylglucosaminyltransferase, and Sys1, a receptor for Arl3, for new markers of *cis*, medial, and *trans* cisternae, respectively (Jungmann and Munro 1998, Yoko-o et al. 2003, Behnia et al. 2004). Mnn9 and Gnt1 are type II transmembrane glycosyltransferases and have a Vps74 recognition motif at their N-termini. Vps74 packs them into COPI-coated vesicles for recycling to early cisternae and controls their steady-state distributions (Tu et al. 2008). Sys1 has been shown to act as a transmembrane receptor for Arl3, but its retention is independent of Vps74 (Schmitz et al. 2008). These resident proteins and commonly used Golgi cisternae markers, Sed5, a t-SNARE (soluble *N*-ethylmaleimide-sensitive factor attachment protein receptor) molecule mostly residing in the *cis* cisternae (Hardwick and Pelham 1992), and Sec7, the guanine-nucleotide exchange factor for Arf GTPase, peripherally associated with *trans*-cisternae and TGN (Achstetter et al. 1988), were tagged with green or red fluorescent proteins. The degrees of colocalization of these Golgi marker proteins were examined by dual color 3D observation. As shown in Fig. 2A, the two *cis* markers GFP-Sed5 and Mnn9-mCherry showed very high probability of colocalization. The percent colocalization with Mnn9-mCherry for Gnt1-GFP, Sys1-GFP, and Sec7-GFP were about 77%, 26%, and 5%, respectively, consistent with

their medial- and *trans*-cisternal localization (Figs. 2A and B). These results reflect the preferential distribution of Golgi resident proteins to particular Golgi cisternae. Note that segregation of two markers is observed within a colocalizing cisterna by SCLIM (Fig. 2C).

Visualization of cisternal maturation using transmembrane Golgi resident proteins

I next examined cisternal maturation of the Golgi apparatus in detail by using these Golgi resident markers. I conducted simultaneous dual-color 4D observations at time resolution of 8 frames/sec (5.7 sec for a 3D image) by SCLIM (Matsuura-Tokita et al. 2006, Kurokawa et al. 2013). Similar to the case in the cell expressing mRFP-Sed5 and Sec7-GFP (Fig. 3C), early cisternae labeled with Mnn9-mCherry changed their color to those of medial cisternae labeled with Gnt1-GFP or *trans* cisternae / TGN labeled with Sys1-GFP, giving evidence for cisternal maturation via recycling of Golgi resident transmembrane proteins (Figs. 3A and B). I determined the transition period between the intensity peaks for each pair of fluorescent markers on a single cisterna (peak-to-peak time) (Daboussi et al. 2012). The average peak-to-peak time from Mnn9-mCherry (*cis*) to Gnt1-GFP (medial) (38.6 sec ± 11.6, n=17) was shorter than that from Mnn9-mCherry (*cis*) to Sys1-GFP (*trans*) (45.6 sec ± 19.6, n=13) (Figs. 3A and B). The transition period from mRFP-Sed5 (*cis*) and Sec7-GFP (*trans*) (87.8 sec ± 34.0, n=11) was longer than that from Mnn9-mCherry (*cis*) to Sys1-GFP (*trans*) (Figs. 3C and 4B). Even though experimental variability was high, these results were consistent with the spatially ordered distribution of Golgi resident proteins within the Golgi apparatus. High-resolution images during the transition of two fluorescent signals

revealed that later markers of the Golgi cisternae, Gnt1-GFP, Sys1-GFP, and Sec7-GFP, began to accumulate as small punctate structures on the early cisternae and increased their volume to cover entire regions on the membrane. By contrast, the earlier markers, Mnn9-mCherry and mRFP-Sed5 signals showed a gradual reduction (Figs. 3A, B and C and 4B). In addition, I noticed that earlier and later Golgi markers did not completely overlap but rather showed segregation within the maturing cisternae, corroborating that functional domains exist within a Golgi cisterna (see also Fig. 2C). I could not observe transition from Mnn9-mCherry-labeled *cis* cisternae to Sec7-GFP labeled *trans* cisternae, indicating Sec7-GFP begins to accumulate later than the disappearance of Mnn9-mCherry from cisternae. This is consistent with the above finding that Mnn9 rarely colocalized with Sec7 (Figs. 2A and B and 4A). The two *trans* markers Sys1 and Sec7 accumulate on cisternae at different maturation phases; Sec7 comes later than Sys1 (83.0 sec ±21.2, n=9) (Fig. 4B). Time course of Golgi marker proteins is shown in Figure 5.

4D observation of cisternal maturation in temperature-sensitive COPI mutant cells

In the previous report, cisternal maturation was slowed down but was still observed in α-COP temperature-sensitive mutant *ret1-1* cells at the restrictive temperature (Matsuura-Tokita et al. 2006). Because this previous observation was made only in 2D time lapse, I decided to reinvestigate this issue using a much improved 4D imaging system developed in RIKEN, SCLIM, which has high sensitivity and high resolution (Kurokawa et al. 2013).

Both in wild-type and *ret1-1* cells at 25˚C, transition of the fluorescent signals from mRFP-Sed5 to Sec7-GFP was observed within 120 seconds, indicating that efficient cisternal maturation occurred in the cells (Figs. 6A and B). By contrast, in *ret1-1* cells at the restrictive temperature, *cis* cisternae labeled with mRFP-Sed5 did not lose red fluorescence but kept it for more than 400 seconds, and never acquired Sec7-GFP signals (Fig. 6B). The rate of successful Golgi maturation was greatly decreased (11%, 5 out of 55 cisternae) in *ret1-1* cells at the restrictive temperature compared to the permissive temperature (62%, 13 out of 21 cisternae). No significant difference was observed for the wild-type upon temperature shift (Fig. 6C). These observations indicate that COPI function is indispensable for cisternal maturation.

4D observation of cisternal maturation in cells depleted for COPI proteins

To further elucidate the role of COPI proteins in cisternal maturation, I developed cells in which COPI proteins were degraded through an auxin-inducible degron (AID) system. The AID system allows specific protein degradation in the presence of plant hormone auxin in non-plant cells (Nishimura et al. 2009). *Arabidopsis thaliana* E3 ubiquitin ligase TIR1 was constitutively expressed in yeast cells and the *A. thaliana* IAA17 sequence was added as a tag at the C-terminus of Ret1 (α-COP) or Sec21 (γ-COP). These cells are designated Ret1-aid or Sec21-aid cells, respectively, or COPI-aid cells collectively. Expression of IAA17-tagged Ret1 and Sec21 could rescue the growth defects of corresponding temperature-sensitive mutants at the restrictive temperature (Fig. 7A). COPI-aid cells exhibited strong growth defects in the presence of 0.5 mM 1-naphthaleneacetic acid (NAA, a synthetic auxin), whereas they grew

normally as wild-type cells in the absence of NAA (Fig. 7B). More than 80% of IAA17-tagged COPI proteins were degraded upon incubation with 1 mM NAA for 2 hours (Fig. 7D). The effect of auxin-dependent degradation of COPI proteins was reversible, because the growth rates of COPI-aid cells after NAA washout were comparable to that of wild-type cells (Fig. 7C). ER and Golgi precursor forms of a vacuolar protein, carboxypeptidase Y (CPY), accumulated in COPI-aid cells after NAA treatment for 2 hours (Fig. 7D). This indicates that anterograde trafficking is also inhibited 2 hours after NAA treatment. The structures of the ER did not appear to be affected under these conditions (Fig. 8).

Using COPI-aid cells expressing Mnn9-mCherry and Gnt1-GFP, I next examined the effect of COPI protein removal on cisternal maturation. COPI-aid cells were treated with 1 mM NAA for 2 hours. The cisternae labeled with Mnn9-mCherry were sustained and never acquired the Gnt1-GFP signal (Figs. 9A, B and C). The rates of cisternal maturation in COPI-aid cells were significantly reduced by NAA treatment (Fig. 9F). These observations again indicate that COPI function is required for the retrograde flux of Golgi resident proteins and is essential for cisternal maturation of the Golgi apparatus. Intriguingly, functional domains labeled with Mnn9-mCherry and Gnt1-GFP were kept segregated within the cisterna in NAA treated COPI aid cells (Figs. 9D and E), suggesting that COPI function is also necessary for domain dynamics. I next examined the effect of COPI depletion on the behaviors of *trans*-Golgi / TGN marker, Sys1-GFP. Transition from Mnn9-mCherry to Sys1-GFP was also disturbed in the presence of NAA in COPI aid cells (Fig. 10). *cis* cisternae labeled with Mnn9-mCherry

never lost their color (Figs. 10A and B, boxed area 2). Cisternae harboring both Mnn9-mCherry and Sys1-GFP retained both fluorescent signals for a prolonged time (Figs. 10A and B, boxed area 1). These results indicate that the function of COPI is required over the whole maturation process of *cis*-to-*trans* cisternae within the Golgi apparatus.

Reduced movements of the Golgi apparatus in COPI inactivated cells

In the course of our observation of cisternal maturation in *ret1-1* cells and COPI aid cells, I realized that the dynamics of Golgi cisternae was affected upon COPI disruption (Fig. 11). *S. cerevisiae* has single layers of Golgi cisternae scattering and moving around in the cytoplasm. It was recently revealed that the *cis* cisternae of Golgi show repeated approach toward ER exit sites (ERES) (hug and kiss action) (Kurokawa et al. 2014) to capture cargo from the ER. In *ret1-1* cells at restrictive temperature, the movement of Sed5-labeled *cis* cisternae was drastically restricted, whereas that of Sec7-labeled *trans* cisternae was less affected (Fig. 11A). In NAA-treated COPI aid cells, 3D tracking of *cis* and medial cisternae demonstrated remarkable inhibition of the cisternal movement (Fig. 11B). Disruption of actin or microtubule cytoskeletons sensitive to latrunculin A and nocodazole, respectively, did not affect either cisternal maturation or movement (Fig. 12). These results suggest that COPI contributes to the dynamic behavior of Golgi cisternae in *S. cerevisiae*.

Discussion

COPI-dependent recycling of Golgi resident proteins drives cisternal maturation from *cis* to *trans*

Cisternal maturation explains a core mechanism for intra-Golgi traffic (Losev et al. 2006, Matsuura-Tokita et al. 2006, Luini 2011). In a typical model, Golgi cisternae serve as anterograde carriers for secretory cargo and the retrograde transport of Golgi resident proteins executes the change in properties of cisternae called maturation. Direct evidence for cisternal maturation was provided by live imaging of yeast *S. cerevisiae* using fluorescent protein-tagged Golgi resident proteins (Losev et al. 2006, Matsuura-Tokita et al. 2006). I was aware, however, of a caveat in selection of fluorescent marker proteins. For example, a frequently used *trans* Golgi marker, Sec7, is a peripheral membrane protein and its recycling between the cytosol and the membrane cannot be ruled out. SNARE proteins are also convenient markers but as they constitute important transport machinery their behaviors may not represent "resident" Golgi proteins. In this study, I have tried to exploit fluorescence-tagged Golgi resident transmembrane proteins such as enzymes for the new markers, and confirmed that they are also good tools to analyze cisternal maturation. Imaging technology by SCLIM is now able to allow us 4D observation of these fluorescence Golgi cisternal markers at high spatiotemporal resolutions (Kurokawa et al. 2013). I have addressed the roles of COPI in intra-Golgi transport processes and the results indicate that the COPI functions are essential for fulfilling the cisternal maturation. Both a temperature-sensitive defect by *ret1-1* mutation and auxin-induced degradation

of Ret1 or Sec21 led to severe blockade of cisternal maturation in both *cis*-to-medial and medial-to-*trans* steps.

Whether COPI executes its functions in the form of COPI vesicles is still an open question. COPI is also involved in tubule formation in mammalian cells (Yang et al. 2011). Tubular connections were sometimes observed between yeast Golgi cisternae (Matsuura-Tokita et al., 2006; Nakano and Luini, 2010). My observation in this study that small membrane puncta from later cisternae emerge on a maturing cisterna (discussed below) strongly suggests the presence of vesicles there, but at the moment I cannot conclude whether they are single vesicles or clusters of vesicles. Roles for COPI-coated tubules are also possible.

Another important question is how COPI controls selective recycling of distinct Golgi resident proteins to their own cisternae. One of the candidates for regulating the selectivity to specific cisternae would be golgin family proteins, because they are thought to specifically capture vesicles from different organelles, endosomes, the ER, and the Golgi apparatus. For example, Golgin-84 (also known as GOLGA5), GMAP210 (also known as TRIP11), and TMF1 have been shown to capture the Golgi resident proteins in mammalian cells (Wong and Munro 2014). In yeast, Rud3 and Sgm1, orthologs of GMAP210 and TMF1, localize to *cis* and *trans* cisternae, respectively (Munro 2011). Whether selective degradation of these golgin family proteins by the AID system affects intra-Golgi trafficking of resident proteins would be a next question to be examined.

Domains are formed and maintained on Golgi cisternae during cisternal maturation

During cisternal maturation, segregation of early and late Golgi resident proteins was observed in individual cisternae in previous report (Matsuura-Tokita et al. 2006). Here, 4D imaging with higher spatiotemporal resolutions reveals details of the compositional change in maturing individual cisternae (see Fig. 3). At the beginning of the transition of *cis* cisternae marked by Mnn9-mCherry, Gnt1-GFP coming from medial cisternae began to localize to small regions on the *cis* cisternae. These small puncta gradually expanded their area without extensive mixing with the *cis* component and eventually covered the whole cisternae. Similar events were also observed for the cases of Sys1-GFP and Sec7-GFP coming into the *cis*-cisternae. Furthermore, two *cis*-Golgi marker proteins, Sed5 and Mnn9, showed segregated distribution on a single cisterna (Fig. 2C). Such segregation of membrane proteins might be an intrinsic property of the Golgi membrane and would be a key to understand their sorting and dynamic equilibrium. In COPI-depleted cells, domain segregation was still observed but in a fixed fashion (see Fig. 9 and 10), suggesting the involvement of COPI in dynamic mixing of domains. The Rab family of GTPases regulate a variety of steps of membrane trafficking. They show phase-specific localization on the Golgi membrane, which is coordinately controlled by Rab GEF and Rab GAP cascades (Rivera-Molina and Novick 2009, Suda et al. 2013). The cells disrupted for the Rab GAP cascade failed in proper Rab GTPase transition and thus in proper membrane segregation but somehow

continued cisternal maturation (Suda et al. 2013). The significance of membrane domain segregation will need further investigation.

COPI also functions in dynamics of Golgi cisternae

Glick and colleagues showed that inactivation of COPI function by anchoring COPI subunits on mitochondria led to the formation of hybrid Golgi structures, in which both early (Vrg4-GFP) and late (Sec7-DsRed or Kex2-mCherry) Golgi-resident proteins were present (Papanikou et al. 2015). These structures fluctuated rapidly and moved around in the cytoplasm. They maintained the early Golgi marker, but showed repeated loss and gain of late Golgi and TGN makers. Anchored COPI proteins have potential to still interact to the Golgi. In our present study, by contrast, the AID system directly removes COPI proteins from cells and COPI depletion brought about marked inhibition of maturation of *cis*-, medial- and *trans*-Golgi and TGN markers (Figs 9 and 10) as well as remarkable repression of the dynamic movement of Golgi cisternae (Fig. 11). Cisternae labeled with both *cis*-Golgi and medial- Golgi or *trans*-Golgi and TGN markers might be deemed similar to the hybrid Golgi structures of Papanikou et al. (2015). However, they sustained these fluorescent signals and did not show repeated loss and gain behavior in our SCLIM observation. Colocalization of both early and late Golgi-resident proteins in a single cisterna was observed as only transient events during cisternal maturation in wild-type cells. These results suggest that in COPI-depleted cells the amount of COPI proteins is insufficient to recycle Golgi-resident proteins, resulting in intermediate cisternae becoming fixed in the maturation process.

Why the dynamics of cisternae is amazingly disturbed by COPI depletion remains a big question to be addressed. Perhaps dynamic release of COPI vesicles or projection of COPI tubules can affect the balance of individual cisternae. Mathematical modeling might be helpful to test such a possibility. *cis*-Golgi cisternae show repeated approaches toward the COPII- coated area localized at ERES and capture cargo proteins there (hug- and-kiss action; Kurokawa et al., 2014). The dynamic behavior of Golgi cisternae must be a pivotal feature in *S. cerevisiae*, which plays many roles in controlling anterograde and retrograde transport in secretory pathway. Analysis of COPI functions would be again a key to tackle the questions of Golgi dynamics.

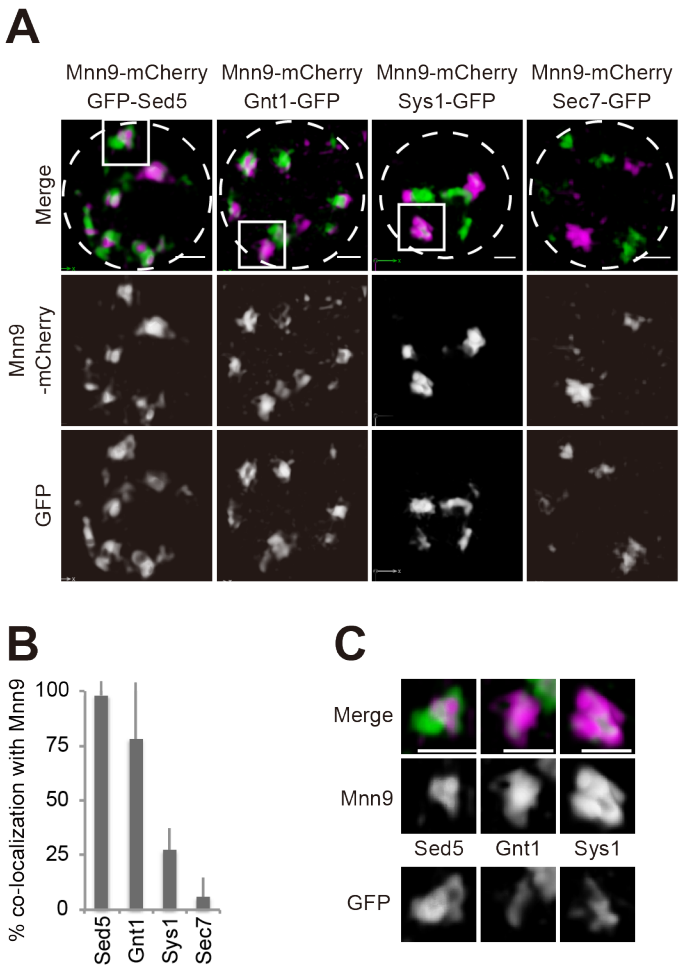

Figure 2 **Localization of Golgi resident proteins.** (A) Localization of Golgi marker proteins with the *cis*-Golgi resident marker Mnn9-mCherry. Wild-type cells expressing GFP-tagged Sed5 (*cis*), Gnt1 (medial), Sys1 (*trans*) and Sec7 (*trans*) with Mnn9-mCherry were grown to a mid-logarithmic phase in synthetic medium at 30°C and observed by 3D confocal fluorescence microscopy. Dashed lines indicate the edge of the cells. (B) Bar graph showing the percentage of Mnn9-mCherry positive cisternae containing GFP-tagged Golgi resident proteins. Error bar indicates SD from 10 independent cells. (C) Enlarged images of the squares in A. Scale bar, 1 μm.

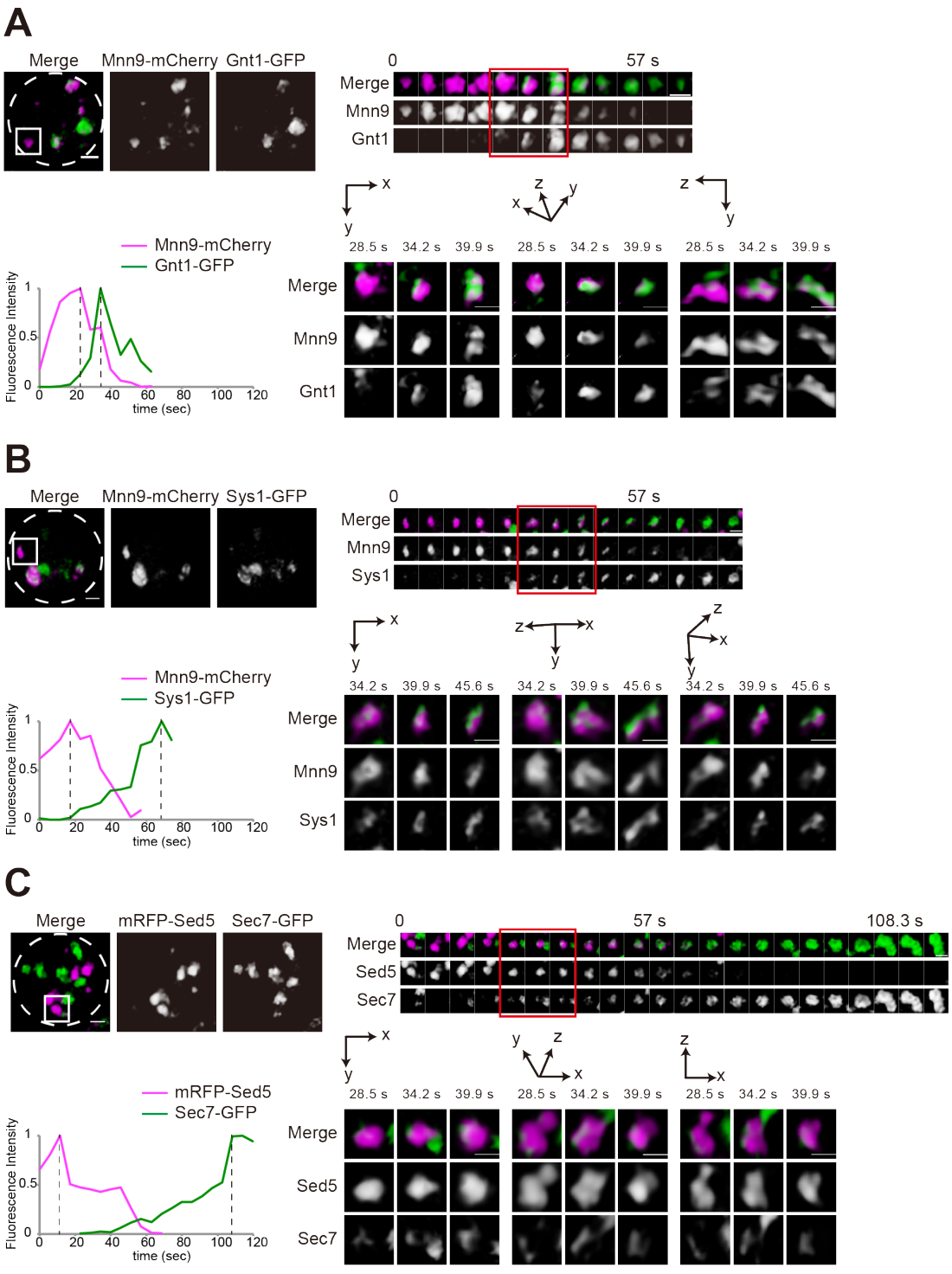

Figure 3 **4D observation of cisternal maturation.** Wild-type cells expressing (A) Mnn9-mCherry (*cis*, magenta) and Gnt1-GFP (medial, green), (B) Mnn9-mCherry (*cis*, magenta) and Sys1-GFP (*trans*, green) and (C) mRFP-Sed5 (*cis*, magenta) and Sec7-GFP (*trans*, green) were grown to a mid-logarithmic phase in synthetic medium at 30˚C and observed by SCLIM. Upper left panel shows representative 3D images.

Dashed lines indicate the edge of the cells. Upper right montages show 3D time-lapse images (4D) of the indicated squares. Lower left shows relative fluorescence intensities of green and red channels in the indicated cisterna. Lower right panel shows magnified images of selected time points from three directions. Scale bar, 1 μm.

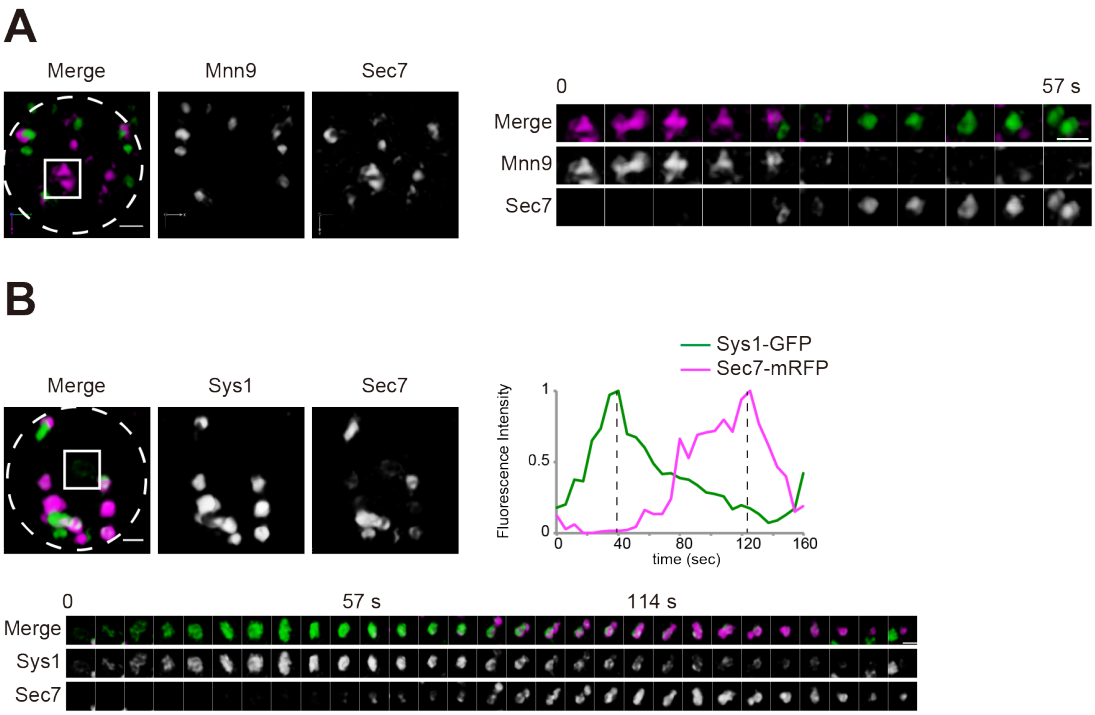

Figure 4 **4D observation of *trans* cisternae markers.** Wild-type cells expressing (A) Mnn9-mCherry (*cis*, magenta) and Sec7-GFP (*trans*, green) and (B) Sys1-GFP (green) and Sec7-mRFP (magenta) were grown to a mid-logarithmic phase in synthetic medium at 30˚C and observed by SCLIM. Dashed lines indicate the edge of the cells. (A) Right panels show 3D time-lapse images (4D) of the indicated squares. (B) Left shows relative fluorescence intensities of green and red channels in the indicated squares. Lower montages show 3D time-lapse images (4D) of the indicated squares. Scale bar, 1 μm.

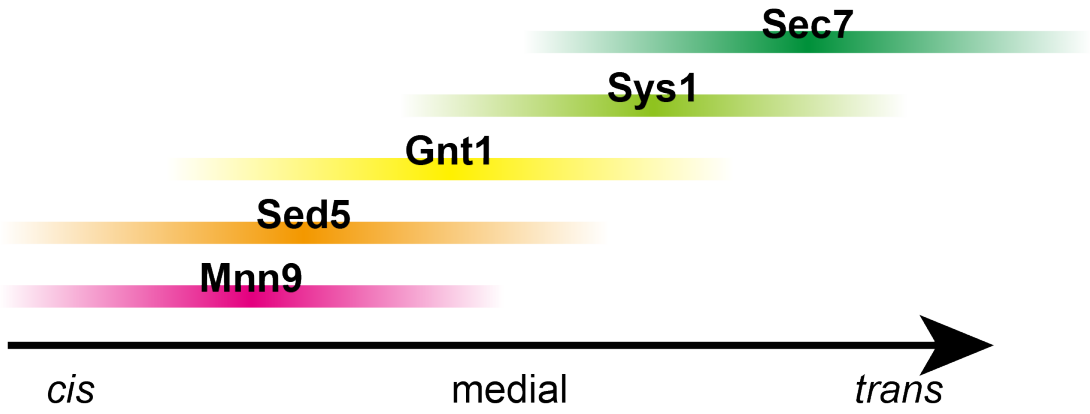

Figure 5 **Time courses of Golgi marker proteins.** Based on the live cell imaging, qualitative time courses of Golgi marker proteins are shown. It takes about 3 minutes to mature from *cis* to *trans*.

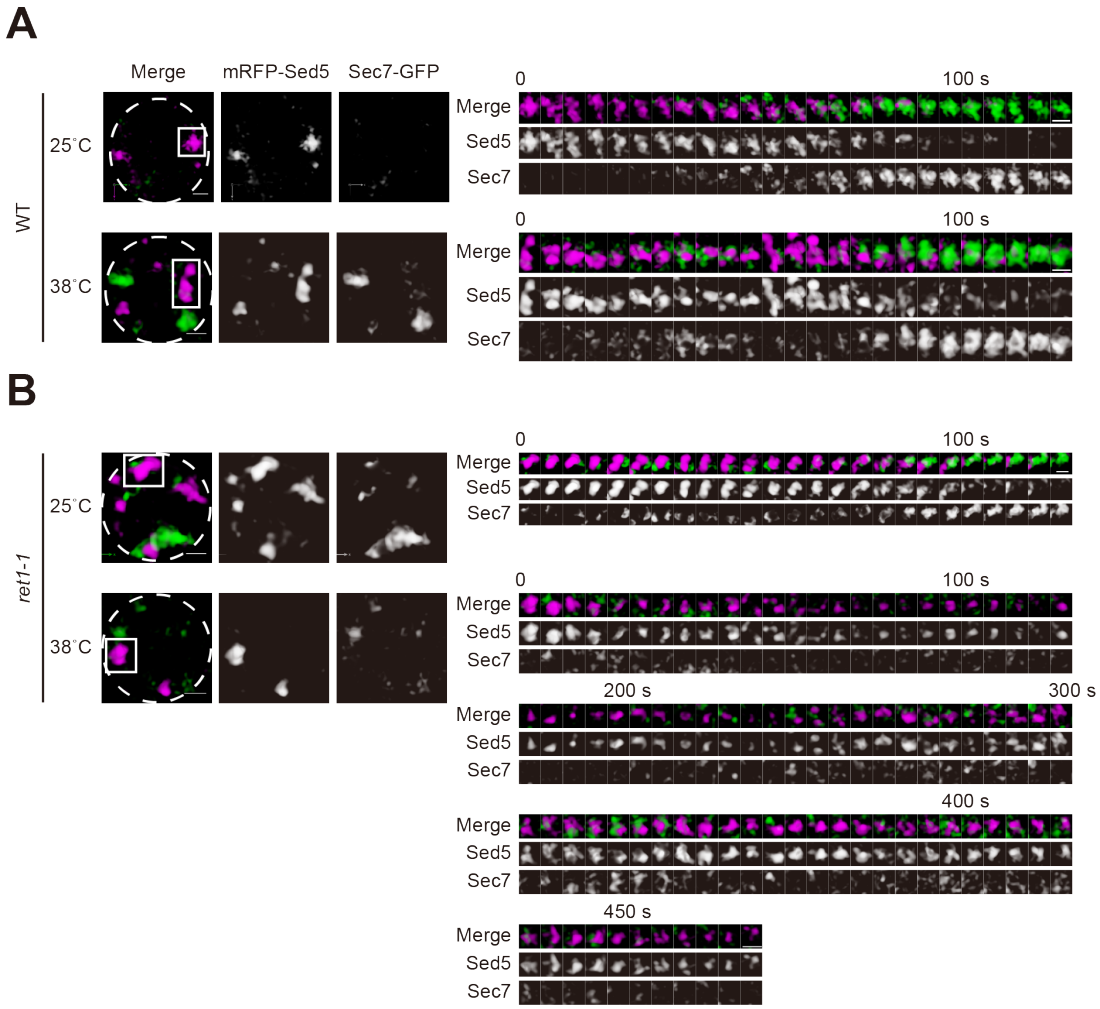

C

	WT		*ret1-1*	
temperature (˚C)	25	38	25	38
matured cisternae	0.70 (12/17)	0.60 (15/25)	0.62 (13/21)	0.11 (5/45)

Figure 6 **4D observation reveals the defect of cisternal maturation in the α-COP mutant *ret1-1* at restrictive temperature.** Wild-type and *ret1-1* cells expressing mRFP-Sed5 (*cis*, magenta) and Sec7-GFP (*trans*, green) were grown to a mid-logarithmic phase in synthetic medium at 25˚C. Wild-type cells cultured at 25˚C and 38˚C for 10 minutes (A) and *ret1-1* cells cultured at 25˚C (permissive) and 38˚C (restrictive) temperature for 10 minutes (B) were observed by SCLIM. Representative 3D images are shown. Dashed lines indicate the edge of the cells. Right montages show 3D time-lapse (4D) images of the indicated squares. Scale bar, 1 μm. (C) The numbers of matured cisternae are shown.

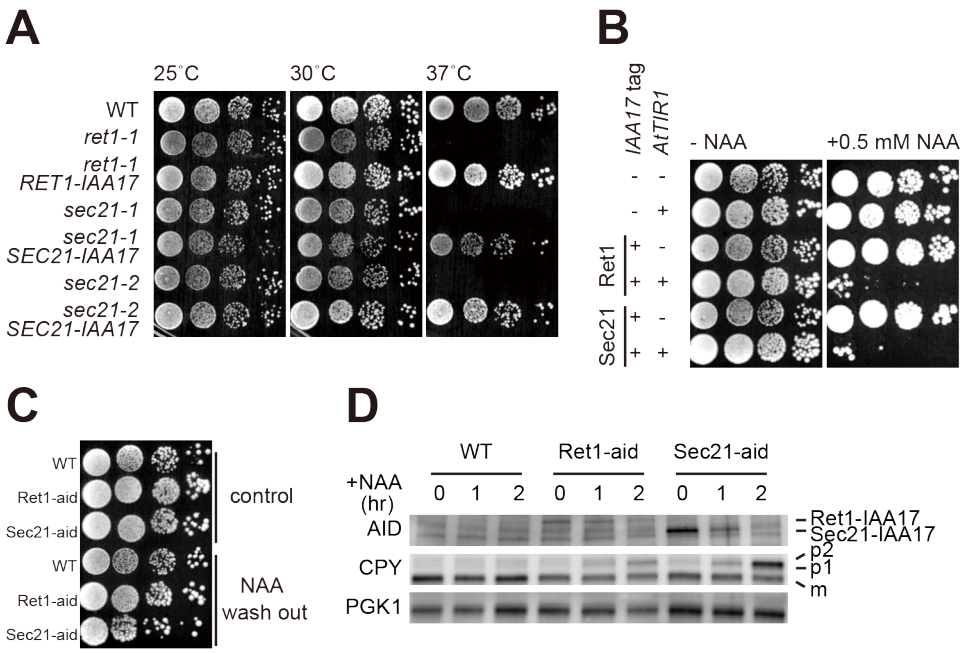

Figure 7 **Degradation of COPI proteins, Ret1 and Sec21, by AID system.** (A) Expression of IAA17-tagged Ret1 and Sec21 by low copy plasmids rescued temperature-sensitive phenotypes of *ret1-1* and *sec21-1* or *sec21-2* cells, respectively. (B) Growth of wild-type, AtTIR1, Ret1-IAA17, Ret1-aid, Sec21-IAA17 and Sec21-aid cells grown on YPD plate with or without 0.5 mM NAA at 30˚C. (C) Growth of NAA-treated cells after NAA washout. Wild-type, Ret1-aid and Sec21-aid cells were cultured in YPD medium with or without 1 mM NAA for 2 hours at 30˚C. After washing out medium with water 3 times, cells were grown on YPD plate at 30˚C. (D) Ret1-aid and Sec21-aid cells were cultured in YPD medium with or without 1 mM NAA at 30˚C. Cells were collected at 0, 1 and 2 hours after NAA addition. Ret1-IAA17, Sec21-IAA17 and CPY proteins were detected by Western blotting. ER form (p1), Golgi form (p2) and mature (m) CPY are indicated on the right. PGK lane shows the loading control.

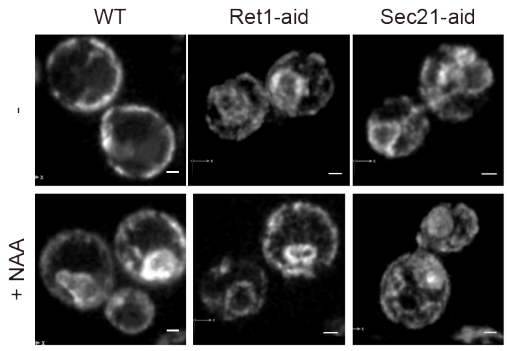

Figure 8 **Observation of ER.** Cells expressing Sec71 transmembrane domain-GFP (ER) were incubated without (upper panels) or with 1 mM NAA (lower panels) for 2 hours. Scale bar, 1 μm.

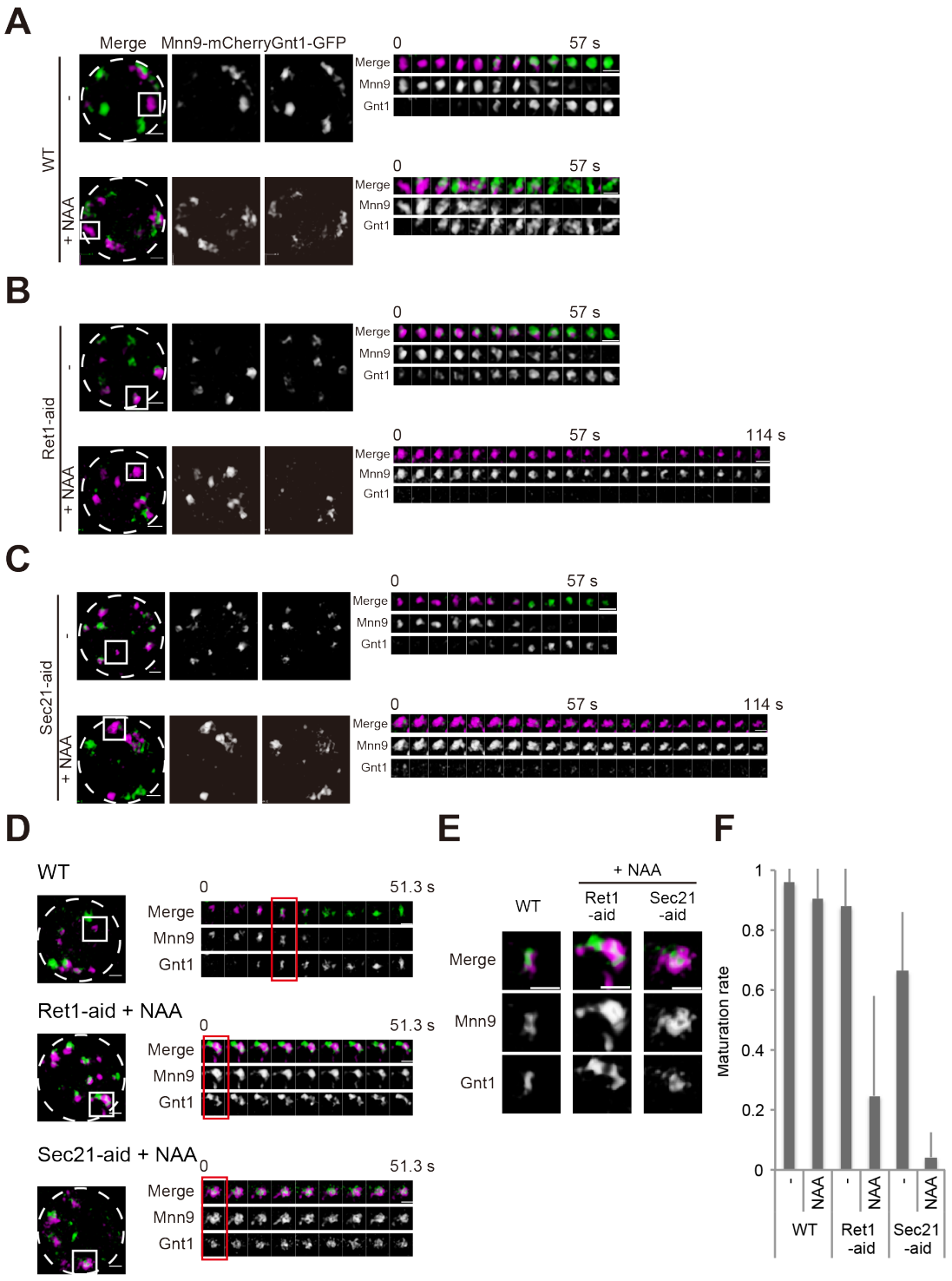

Figure 9 **Depletion of COPI protein inhibits *cis* to medial cisternal maturation.** (A) Wild-type, (B) Ret1-aid, and (C) Sec21-aid cells expressing Mnn9-mCherry (*cis*, magenta) and Gnt1-GFP (medial, green) were grown to a mid-logarithmic phase in synthetic medium with or without 1 mM NAA at 30˚C and observed by SCLIM. Representative 3D images of cells with (lower panels) or without (upper) NAA are

shown. Dashed lines indicate the edge of cells. Right montages show 3D time-lapse images of the indicated squares. (D) Wild-type, Ret1-aid and Sec21-aid cells with NAA expressing Mnn9-mCherry (*cis*, magenta) and Gnt1-GFP (medial, green) were observed. Left panels show representative 3D images of cells. Dashed lines indicate the edge of cells. Right montages show 3D time-lapse images of the indicated squares. (E) Magnified images of selected time points in D are shown. Scale bar, 1 μm. (F) Bar graph shows the rate of matured cisternae from *cis* to medial. Error bars represent SD from at least 5 independent cells.

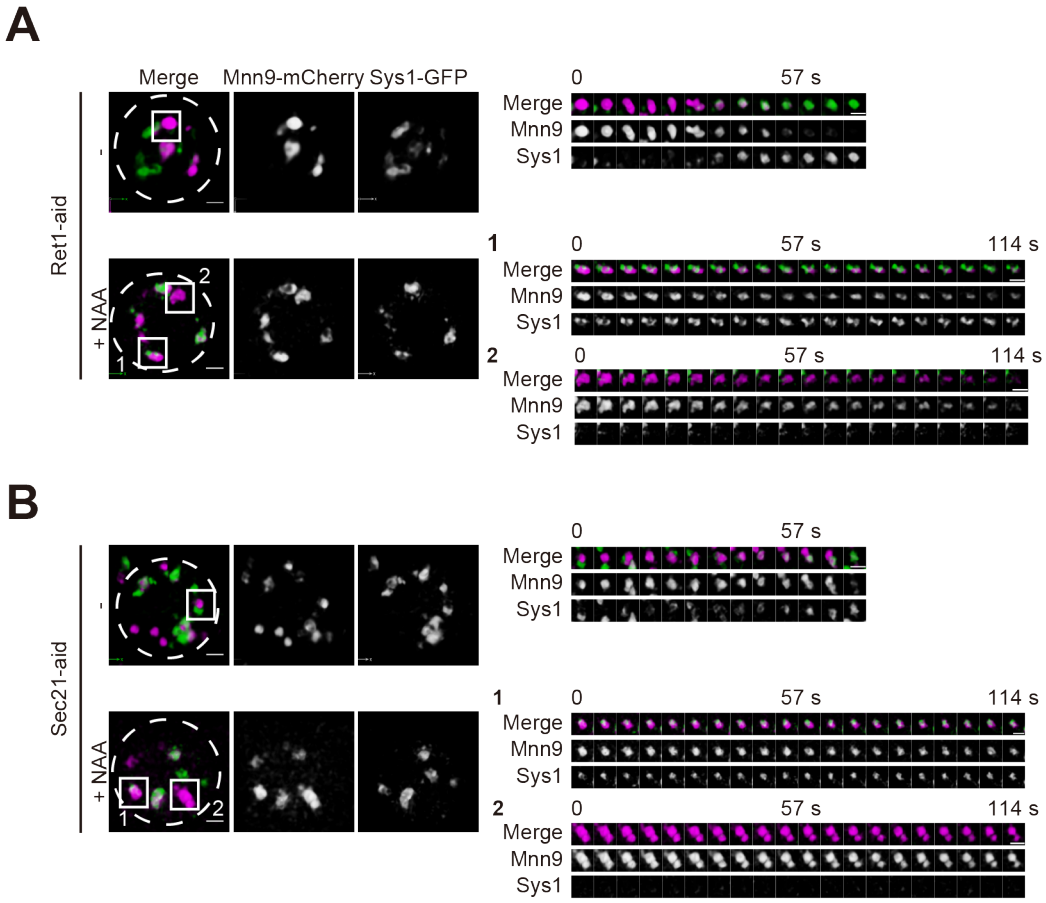

Figure 10 **Depletion of COPI protein inhibits *cis* to *trans* cisternal maturation.** Ret1-aid (A) and Sec21-aid (B) cells expressing Mnn9-mCherry (*cis*, magenta) and Gnt1-GFP (medial, green) were grown to a mid-logarithmic phase in synthetic medium with or without 1 mM NAA at 30˚C and observed by SCLIM. Representative 3D images of cells with (lower panels) or without (upper) NAA are shown. Dashed lines indicate the edge of cells. Right panels show 3D time-lapse images of the indicated squares. Scale bar, 1 μm.

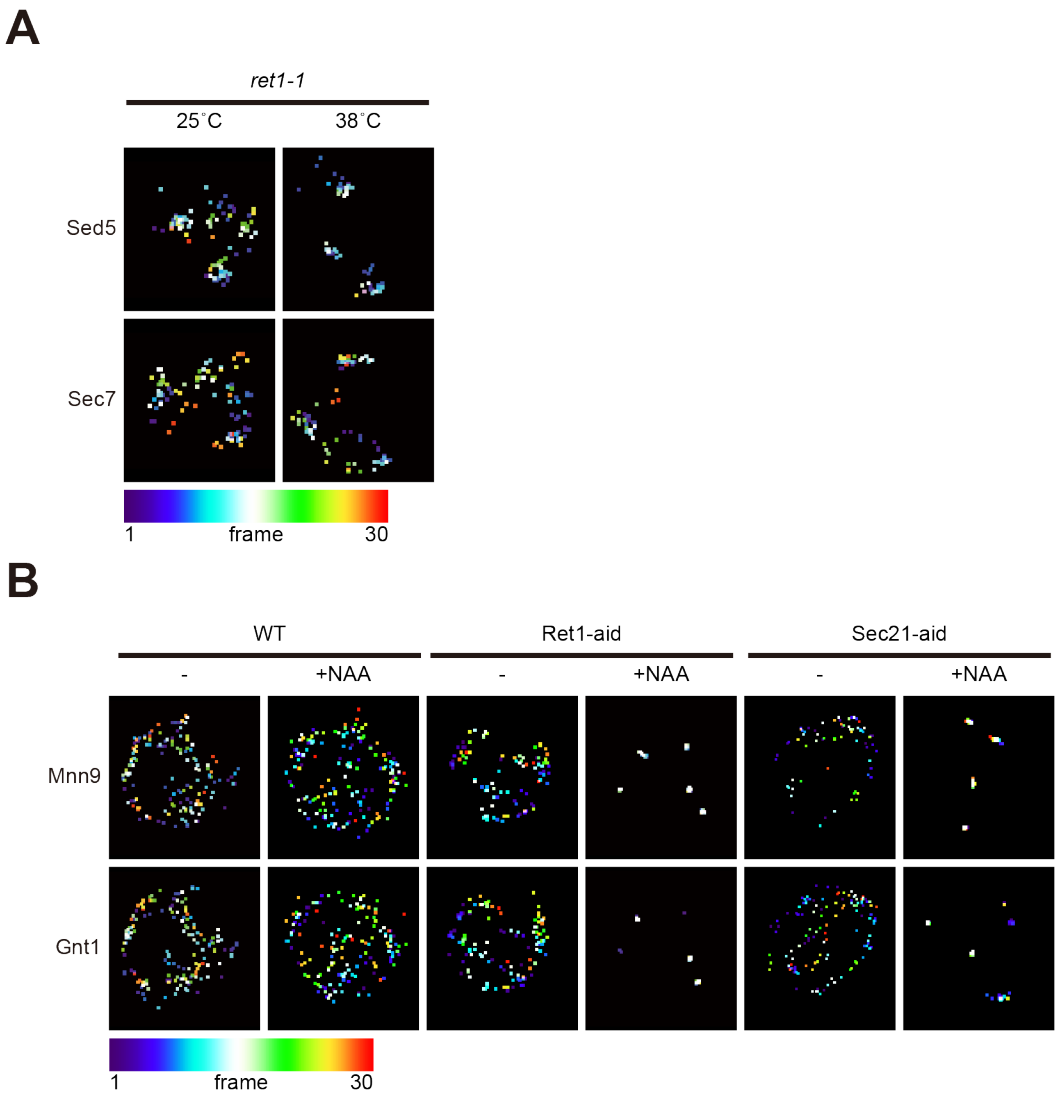

Figure 11 **Inhibition of COPI functions reduced cisternal movement.** The z and time projections of center of mass of each cisterna are shown. The colors of points indicate the time point shown at bottom left. (A) Images of *ret1-1* cells expressing mRFP-Sed5 (*cis*) and Sec7-GFP (*trans*) at 25˚C and 38˚C were processed. One z-stack was collected every 5 sec. (B) Images of wild-type, Ret1-aid and Sec21-aid cells expressing Mnn9-mCherry (*cis*) and Gnt1-GFP (medial) with or without 1 mM NAA for 2 hours were processed. Z-stack images were collected for every 5.7 sec.

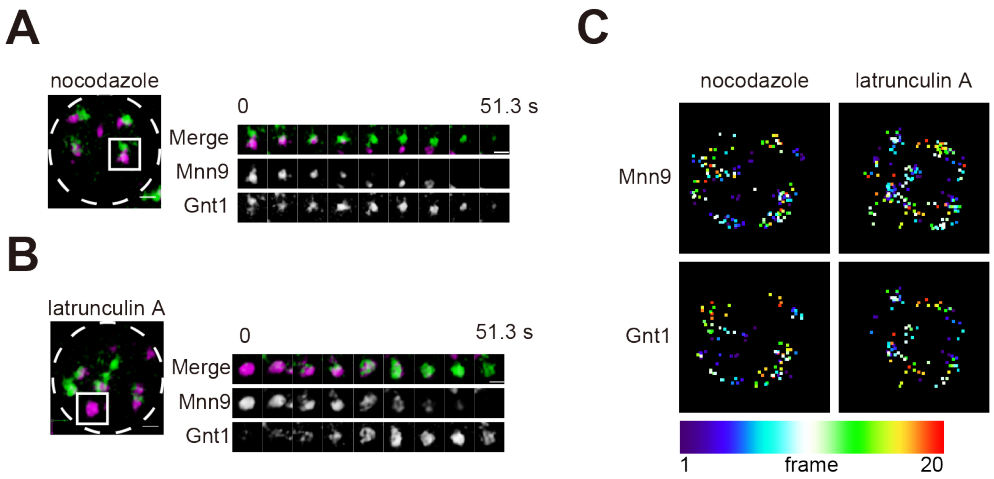

Figure 12 **Effects of depolymerization of microtubules and actin filaments on cisternal maturation and dynamics.** Wild-type cells expressing Mnn9-mCherry (*cis*, magenta) and Gnt1-GFP (medial, green) were grown to a mid-logarithmic phase in synthetic medium at 30°C, treated with (A) 50 μg/mL Nocodazole for 20 minutes and (B) 200 μM Latrunculin A for 3 minutes, and observed by SCLIM. Dashed lines indicate the edge of the cells. Right montages show 3D time-lapse (4D) images of the indicated squares. Scale bar, 1 μm. (C) The z and time projections of center of mass of each cisterna in A and B are shown. The colors of points indicate the time point shown at bottom left. Left images show cells expressing Mnn9-mCherry (*cis*) and Gnt1-GFP (medial). One z-stack was collected every 5.7 sec.

Chapter 2

本章については５年以内に雑誌等で観光予定の刊行予定のため予定のため、
非公開。

Materials and Methods

Yeast strains and plasmids

Yeast strains, plasmids and primers used in this study are listed in Table. S1, S2 and S3, respectively. *ADE2+* cells were made by integration with pRS402 (Brachmann et al. 1998) digested by *Stu*I into the *ade2* site. mRFP-Sed5 and Sec7-GFP were co-expressed under the control of *TDH3* promoter for mRFP-Sed5 and *ADH1* promoter for Sec7-GFP on the low-copy plasmid pRS316 (Matsuura-Tokita et al. 2006). Gnt1-GFP and Sys1-GFP were expressed under the control of *ADH1* promoter and *CMK1* terminator on the low-copy plasmids, pRS316 or pRS314 (Sikorski and Hieter 1989). These plasmids were constructed in several steps. First, the DNA fragment containing *ADH1* promoter or *CMK1* terminator obtained from yeast genomic DNA by PCR with appropriate sets of primers, SacI-ADH1p-F and ADH1p-NotI-R, or XhoI-CMK1t-F and CMK1t-SacI-KpnI-R, was subcloned into the *Sac*I-*Not*I or *Xho*I-*Kpn*I sites of pRS316, respectively to produce pRS316-ADH1p-CMK1t. Next, the DNA fragment of *GFP* obtained from pSKY5 (Sato et al. 2001) by PCR with primers, SalI-GFP-F and GFP-XhoI-R was subcloned into the *Sal*I-*Xho*I sites. Then, the DNA fragment of *GNT1* or *SYS1* obtained from yeast genomic DNA by PCR with primers, NotI-GNT1-F and GNT1-SalI-R or XbaI-SYS1-F and SYS1-HindIII-R was subcloned into the *Not*I-*Sal*I sites or *Xba*I-*Hin*dIII sites of pRS316 harboring *ADH1* promoter, *GFP* and *CMK1* terminator to develop pRS316-ADH1p-GNT1-GFP-CMK1t or pRS316-ADH1p-SYS1-GFP-CMK1t, respectively.

pRS316-ADH1p-GNT1-GFP-CMK1t was digested by *Sac*I and subcloned into the *Sac*I

site of pRS314 to produce pRS314-ADH1p-GNT1-GFP-CMK1t. pRS316-ADH1p-SYS1-GFP-CMK1t was digested by *Pvu*II and subcloned between the *Pvu*II sites of pRS314 to produce pRS314-ADH1p-SYS1-GFP-CMK1t. pRS304-SEC71TMD-GFP was constructed by subcloning the DNA fragment between *Pvu*II sites of pRS306-SEC71TMD-GFP (Sato et al. 2003) into pRS304 (Sikorski and Hieter 1989). Strains expressing Sec71TMD-GFP were constructed by the integration with DNA fragment of pRS304-SEC71TMD-GFP digested by *Bsu*36I into the *trp1* site of yeast genome. Strains expressing fluorescent protein-tagged Mnn9 were constructed by a PCR-based method described in a previous report (Kurokawa et al. 2014).

Strains expressing IAA17-tagged Ret1 and Sec21 at their carboxyl-termini were constructed by a PCR-based method using pMK43 plasmid as a template (Nishimura et al. 2009) and primers (RET1-S2 and RET1-S3 for aid-tagged *RET1* and SEC21-S2 and SEC21-S3 for aid-tagged *SEC21*). *Arabidopsis thaliana* E3 ubiquitin ligase TIR1 was expressed by pMK76 integrated into the *ura3* site of each yeast genome by *Stu*I digestion (Nishimura et al. 2009).

The DNA fragment coding *FIS1* was obtained from yeast genomic DNA by PCR with the primers (KpnI-FIS1-F and FIS1w/Stop-NotI-R), digested by *Kpn*I and *Not*I and subcloned into the *Kpn*I-*Not*I sites of pYES2 to produce pYES2-FIS1. The DNA fragment coding mCherry was obtained from pFA6a-mCherry-natNT2 (Kurokawa et al. 2014) by PCR with the primers (BamHI-xFP_inpYES2_InFu-Fwd and xFP-BamH_inpYES2_InFu-Rev) and subcloned into *Kpn*I digested pYES2-FIS1 by In-Fusion cloning (Takara) to produce pYES2-mCherry-FIS1. DNA fragment coding

COG2, *COG3*, *COG4* and *COG5* were obtained from yeast genomic DNA by PCR with the primers (HindIII-COG2-F, COG2w/oStop-KpnI-R for COG2, HindIII-COG3-F, Cog3w/oStop-KpnI-R for COG3, HindIII-COG4-F, COG4w/oStop-KpnI-R for COG4 and HindIII-COG5-F, COG5w/oStop-KpnI-R for COG5), digested by *Hin*dIII and *Kpn*I and subcloned into the *Hin*dIII-*Kpn*I sites of pYES2-mCherry-FIS1 to produce pYES2-COG2, 3, 4 and 5-mCherry-FIS1. The DNA fragment coding *COG1*, *COG6*, *COG7* and *COG8* were obtained from yeast genomic DNA by PCR with the primers (HindIII-COG1 in pYES2 InFu-Fwd, COG1w/oStop-KpnI in pYES2-mCh-FIS1 InFu-Rev for COG1, HindIII-COG6 in pYES2 InFu-Fwd, COG6w/oStop-KpnI in pYES2-mCh-FIS1 InFu-Rev for COG6, HindIII-COG7 in pYES2 InFu-Fwd, COG7w/oStop-KpnI in pYES2-mCh-FIS1 InFu-Rev for COG7 and HindIII-COG8 in pYES2 InFu-Fwd, COG8w/oStop-KpnI in pYES2-mCh-FIS1 InFu-Rev) and subcloned into *Hin*dIII and *Kpn*I digested pYES2-mCherry-FIS1 by In-Fusion cloning to produce pYES2-COG1, 6, 7 and 8-mCherry-FIS1. pYES2-COG-mCherry-FIS1s were digested with *Bam*HI to remove mCherry and self-ligated to produce pYES2-COG-FIS1s.
The DNA fragments of GAL1pr-COG4, 5, 6, 7 and 8-mCherry-FIS1-CYC1term were obtained from pYES2-COG4, 5, 6, 7 and 8-mCherry-FIS1 respectively by PCR with primers (SacII-GAL1p-F, CYC1term-SalI-R), digested by *Sac*II and *Sal*I and subcloned into *Sac*II-*Sal*I sites of pRS306 to produce pRS306-GAL1pr-COG4, 5, 6, 7, and 8-mCherry-FIS1-CYC1term. The DNA fragments of GAL1pr-COG1, 2 and 3-mCherry-FIS1-CYC1term were obtained from pYES2-COG1, 2 and 3-mCherry-FIS1 respectively by PCR with primers (SacII-GAL1p-F, CYC1t-SmaI-R), digested by *Sac*II

and *Sma*I and subcloned into *Sac*II-*Sma*I sites to produce pRS306-GAL1pr-COG1, 2 and 3-mCherry-FIS1-CYC1term.

The DNA fragment coding *COG1* and *COG3* were obtained from yeast genomic DNA by PCR with primers (NotI-COG1-F, COG1w/Stop-XhoI-R for COG1 and NotI-COG3-F, COG3w/Stop-XhoI-R for COG3), digested by *Not*I and *Xho*I subcloned into the *Not*I-*Xho*I sites of pYES2 to produce pYES2-COG1 and pYES2-COG3. The DNA fragment coding *COG2* was obtained from yeast genomic DNA by PCR with primers (HindIII-COG2-F, COG2w/Stop-KpnI-R), digested by *Hin*dIII and *Kpn*I and subcloned into *Hin*dIII-*Kpn*I sites of pYES2 to produce pYES2-COG2. The DNA fragments coding *COG4* was obtained from yeast genomic DNA by PCR with primers (HindIII-COG4-F, COG4w/Stop-XhoI-R), digested by *Hin*dIII and *Xho*I and subcloned into *Hin*dIII-*Xho*I sites of pYES2 to produce pYES2-COG4. The DNA fragments coding *COG5*, *COG6*, *COG7* and *COG8* were obtained from yeast genomic DNA by PCR with primers (BamHI-COG5-F, COG5w/Stop-SalI-R for COG5, BamHI-COG6-F, COG6w/Stop-SalI-R for COG6, BamHI-COG7-F, COG7w/Stop-SalI-R for COG7 and BamHI-COG8-F, COG8w/Stop-SalI-R for COG8), digested by *Bam*HI and *Sal*I and subcloned into *Bam*HI-*Xho*I sites of pYES2 to produce pYES2-COG5, pYES2-COG6, pYES2-COG7 and pYES2-COG8.

The DNA fragment coding 13Myc-*ADH1*terminator was obtained from pFA6a-13Myc-KanMX6 (Longtine et al. 1998) by PCR with primers (XhoI-Myc-F, ADH1t-KpnI-R), digested by *Xho*I and *Kpn*I and subcloned into *Xho*I-*Kpn*I sites of

pRS304 (Sikorski and Hieter 1989) to produce pRS304-13Myc-ADH1term. The DNA fragment coding *SUC2* was obtained from yeast genome DNA by PCR with primers (SacI-SUC2-F, SUC2w/oStop-XhoI-R), digested by *Sac*I and *Xho*I and subcloned into *Sac*I-*Xho*I sites of pRS304-13Myc-ADH1term to produce pRS304-SUC2-13Myc-ADH1term. SUC2-13Myc expressing cells were constructed by the integration with DNA fragment of pRS304-SUC2-13Myc-ADH1term digested by *Bam*HI into the *SUC2* site of yeast genome.

Gene disruptions of COG subunits (YPH499 background) were constructed by a PCR-based methods using *cog5, 6, 7 and 8::kanMX6* (BY4741, Invitrogen) genome DNA as templates with primers (COG5upATG200b-F, COG5downStop200b-R for cog5Δ, COG6upATG100b-F, COG6downStop100b-R for cog6Δ, COG7upATG200b-F, COG7downStop200b-R for cog7Δ and COG8upATG100b-F, COG8downStop100b-R for cog8Δ).

pRS306-GAL1p-COG1-mCherry-FIS1, pRS306-GAL1p-COG2-mCherry-FIS1, pRS306-GAL1p-COG3-mCherry-FIS1, pRS306-GAL1p-COG4-mCherry-FIS1, pRS306-GAL1p-COG6-mCherry-FIS1 and pRS306-GAL1p-COG8-mCherry-FIS1 were digested by *Nde*I and integrated into the *ura3* site of the yeast genome. pRS306-GAL1p-COG5-mCherry-FIS1 was digested by *Eco*RV and integrated into the *ura3* site of the yeast genome. pRS306-GAL1p-COG7-mCherry-FIS1 was digested by *Bst*BI and integrated into the *ura3* site of the yeast genome.

The DNA fragment coding GFP was obtained from pSKY5 by PCR with primers (NotI-xFP-F, xFPw/oStop-XbaI-R), digested by *Not*I and *Xba*I and subcloned

into *Not*I-*Xba*I sites of pRS316-ADH1p-CMK1t to produce pRS316-ADH1p-GFP(N)-CMK1. The DNA fragment coding *TLG1* was obtained from yeast genomic DNA by PCR with primers (BamHI-TLG1-F, TLG1w/Stop-EcoRI-R), digested by *Bam*HI and *Eco*RI and subcloned into *Bam*HI-*Eco*RI sites of pRS316-ADH1p-GFP(N)-CMK1t to produce pRS316-GFP-TLG1. pRS316-GFP-SED5, pRS316-GFP-GOS1 or pRS316-GFP-TLG1 were digested by *Pvu*I and transformed with *Eco*RI digested pRS314.

Microscopy

Fluorescence microscopy was performed by super-resolution confocal microscopy (SCLIM). The system setup had an Olympus model IX-71 inverted fluorescence microscope with a UPlanSApo 100 X NA 1.4 oil objective lens (Olympus, Japan), a high-speed spinning-disk confocal scanner (Yokogawa Electric, Japan), a custom-made spectroscopic unit, image intensifiers (Hamamatsu Photonics, Japan) with a custom-made cooling system, and two EM-CCD cameras (Hamamatsu Photonics, Japan) for green and red channels (Kurokawa et al. 2013). For microscopic observation, all strains were grown in selective medium (0.67% yeast nitrogen base without amino acids and 2% glucose) with appropriate supplements. *ret1-1* mutant cells were cultured at permissive temperature (25˚C) and then incubated at restrictive temperature (38˚C) for 10 minutes on a thermo-controlled stage (Tokai Hit, Japan) whose temperature was kept at 38˚C. Ret1-aid cells and Sec21-aid cells were grown with 1 mM NAA for 2 hours. For 4D live imaging of wild-type cells, Ret1-aid cells, and Sec21-aid cells, 32 optical slices spaced 0.1 μm apart were sequentially collected at 8 frames per second

(fps), which takes 5.7 seconds in total including the time for data transfer. For 4D observation of *ret1-1* mutant cells, 32 optical slices 0.1 μm apart were collected at 15 fps every 5 seconds. Z stack images were converted to 3D voxel data and processed by iterative deconvolution with Volocity (Perkin Elmer) using theoretical point-spread function for spinning-disc confocal microscopy. Maximum intensity projection images from these deconvolved 3D images were used for the calculation of relative fluorescent values of green and red signals of the Golgi areas by Fiji software (Schindelin et al. 2012). Center of mass of each cisterna was calculated in a mask of the cisterna from raw 4D images by Fiji software. Projection of center of mass was conducted by Temporal-Color Code of Fiji plugin with thermal lookup table.

For imaging of COG-mCherry-Fis1 cells, 42 optical slices spaces 0.1 μm apart were collected. Maximum intensity projection was conducted by z project of Fiji plugin Max Intensity.

Western blotting for COPI-aid cells

Cells expressing aid-tagged proteins were cultured in YPD (1% yeast extract, 2% peptone, and 2% glucose) medium at 30˚C for overnight. Yeast culture was inoculated in fresh medium and grown until OD_{600} = 0.5. 0.5 OD_{600} unit cells were collected for loading sample. Cultures were incubated at 30˚C for 1 or 2 hours with or without 1 mM NAA and were collected for loading samples at 1 or 2 hours with or without NAA. 0.5 OD_{600} unit cells were suspended in 100 μl Laemmli's Sample buffer and then disrupted by vortex with glass beads. The cell suspensions were boiled at 100˚C for 5 minutes and cleared by centrifugation at 15,000 rpm for 5 minutes to

prepare total cell lysates. Proteins corresponding to 5 μl of total cell lysates were analyzed by SDS/PAGE, followed by Western blotting with anti-AID antibody (1: 2000, BioROIS CO.), anti-CPY antibody (1:3000, rabbit, polyclonal) (Yahara et al. 2001) and anti-PGK antibody (1:10000, 22C5, Invitrogen). Bands were visualized by horseradish peroxidase-conjugated sheep anti-mouse IgG and donkey anti-rabbit IgG antibodies (GE healthcare).

COG-GFP Pull Down

Endogenous COG1, 3, 5 and 6 were tagged with GFP at C-termini (Invitrogen GFP clones, BY4741 background). Cells were grown at 30˚C to an OD_{600} of ~1.0 in YPD medium (1% yeast extract, 2% polypeptone, 2% glucose). 200 OD_{600} unit cells were harvested and washed with water. The pellet was resuspended in 5 mL of 0.1 M Tris-HCl (pH9.4)/ 10 mM DTT, incubated at 30˚C for 10 minutes, harvested, resuspend in 5 mL of 50 mM HEPES pH7.2/ 0.8 M mannitol/ 20 μL zymolyase, and spheroplasted for 1 hour at 30˚C. Spheroplasts were harvested by centrifugation at 2,000 x g 5 minutes at room temperature and washed with 50 mM HEPES pH7.2/ 0.8 M mannitol. The pellet was resuspend in 20 mL of YPD with 0.8 M mannitol and incubated for 90 minutes at 30˚C. Cells were harvested by centrifugation at 2,000 x g for 5 minutes at room temperature, washed with 50 mM HEPES pH7.2/ 0.8 M mannitol. Cells were resuspended 1 mL of IP buffer [150 mM NaCl/ 50 mM Tris (pH7.4)/ 7 μL/mL Halt Protease Inhibitor Cocktail EDTA free (Thermo Fisher)/ 1 mM PMSF] and homogenized by dounce homogenizer. Total cell lysates were centrifuged at 2,000 x g for 5 minutes at 4˚C to remove debris. Supernatants were separated into supernatant

(cytosol) and pellet (membrane) fraction by ultracentrifugation at 100,000 x g for 1 hour at 4˚C in a Beckman Optima MAX-XP Ultracentrifuge (TLA 55 rotor). Pellet was resuspended in 500 μL of IP buffer containing 1% Triton X-100, incubated on ice for 30 minutes and centrifuged at 10,000 x g for 5 minutes at 4˚C. Supernatant (detergent soluble membrane fraction) was used as membrane fraction (P100) for the following immunoprecipitation analysis. 500 μL of supernatant (S100, cytosol fraction) was solubilized with Triton X-100 (final concentration 1%) on ice for 30 minutes. 1 μL of anti-GFP antibody (mouse monoclonal, 3E6, Thermo Fisher) was added to both membrane and cytosol fractions and incubated on ice in a cold room over night. 60μL of 30% Protein G beads (Protein G-Agarose, Roche) was added to each tubes and incubated with gentle mixing in a cold room for 2 hours. Beads were then washed four times with PBS containing 0.05% Triton. Samples were eluted in 2x Laemmli sample buffer (Bio-Rad) and heated for 5 minutes at 95˚C to elute the bound proteins.

mCherry beads Immunoprecipitation

GAL1prCOG-mCherry-Fis1s were integrated at *ura3* site of the yeast chromosome (YPH499 background). Cells were grown at 30˚C in SD with galactose medium (1.7% yeast nitrogen base without amino acid and ammonium sulfate, 5% ammonium sulfate, 2% dropout supplement mixture –uracil, 2% galactose) over night. 200 OD_{600} unit cells in log phase were harvested and washed with water. The pellet was resuspended in 5 mL of 0.1 M Tris-HCl (pH9.4)/ 10 mM DTT, incubated at 30˚C for 10 minutes, harvested, resuspend in 5 mL of 50 mM HEPES pH7.2/ 0.8 M mannitol/ 20 μL zymolyase, and spheroplasted for 1 hour at 30˚C. Spheroplasts were harvested by

centrifugation at 2,000 x g 5 minutes at room temperature. Spheroplasts were resuspend 1 mL of IP buffer and homogenized by dounce homogenizer. Total cell lysates were centrifuged at 2,000 x g for 5 minutes at 4˚C to remove debris. Triton X-100 (final concentration 1%) was added to supernatant and incubated on ice to solubilize. 60 μL of 50% mCherry-Nanobody beads (LaM4.2-His beads) (Fridy et al. 2014) was added and incubated with gentle mixing at room temperature for 1.5 hour. Beads were then washed four times with PBS containing 0.05% Triton. Samples were eluted in 2x Laemmli sample buffer (Bio-Rad) and heated for 5 minutes at 95˚C to elute the bound proteins.

Western blotting for COG-GFP Pull Down and mCherry beads Immunoprecipitation

Samples were analyzed by SDS/PAGE, followed by Western blotting with primary mouse monoclonal antibody (anti-GFP (1: 1000, B34, COVANCE)), rabbit polyclonal antibodies (anti-COG1, 3-8 (1: 1000) and anti-COG2 (1: 250) (Fotso et al. 2005), anti-mCherry (1: 500, Lupashin Lab.)). Bands were visualized by appropriate secondary antibodies conjugated with IRDye 680 or IRDye 800 dyes (LI-COR).

Western blotting for CPY and invertase

Cells expressed COG-mCherry-Fis1 by chromosomal integration plasmids were cultured in YPGalSuc (1% yeast extract, 2% peptone, 1% galactose and 1% sucrose) over night at 30˚C. Cells expressed COG-mCherry-Fis1 by multi copy plasmids were cultured in selective medium (0.67% yeast nitrogen base without amino acids, 1% raffinose) with appropriate supplements over night and then in selective medium (0.67% yeast nitrogen base without amino acids, 2% galactose) with

appropriate supplements for 5 hours at 30˚C. 1 OD_{600} unit cells were harvested and resuspend in 100 μL in Laemmli's sample buffer and then disrupted by vortex with glass beads. The cell suspensions were boiled at 100˚C for 5 minutes. Proteins corresponding to 5 μl of total cell lysates were analyzed by SDS/PAGE, followed by Western blotting with anti-CPY antibody (1:3000, rabbit, polyclonal) (Yahara et al. 2001) and anti-c-Myc (1: 2000, 9E10, COVANCE). Bands were visualized by horseradish peroxidase-conjugated sheep anti-mouse IgG and donkey anti-rabbit IgG antibodies (GE healthcare).

Subcellular fractionation

Cells expressing COG-mCherry-Fis1 by multi copy plasmids were cultured in selective medium (0.67% yeast nitrogen base without amino acids and 2% glucose) with appropriate supplements over night and then in selective medium (0.67% yeast nitrogen base without amino acids and 2% galactose) with appropriate supplements for 5 hours at 30˚C. 2 OD_{600} unit cell cells were harvested and resuspend in 100 μL Lysis buffer [50 mM KOAc/2 mM EDTA/20 mM Hepes-KOH (pH6.8)/1 mM DTT 20 μg/ml PMSF/ c0mplete mini EDTA-free (Roche)] and disrupted by vortex with glass beads. The cell lysates were centrifuged at 300 x g for 5 minutes at 4˚C to remove debris. Supernatants were separated into supernatant (S13) and pellet (P13) fraction by centrifugation at 13,000 x g for 15 minutes at 4˚C. P13 fraction was washed with 500 μL Lysis buffer and resuspended in 50 μL Lysis buffer. 50 μL 2x Laemmli's sample buffer was added to total, S13 and P13 fractions. Samples were boiled at 100˚C for 5 minutes. Proteins corresponding to 5 μL of total cell lysates were analyzed by

SDS/PAGE, followed by Western blotting with anti-Och1 (1:3000, rabbit polyclonal) (Hirata et al. 2013), anti-Sed5 (1:1000, rabbit polyclonal) (Sato and Nakano 2003), anti-PGK antibody (1:10000, 22C5, Invitrogen) and anti-Porin (1:500, 16G9, Invitrogen). Bands were visualized by horseradish peroxidase-conjugated sheep anti-mouse IgG and donkey anti-rabbit IgG antibodies (GE healthcare).

Table 1 Strains used this study

Name	Genotype	Background	Source
YPH499	*MAT***a** *ura3-52 lys2-801 ade2-101 trp1-D63 his3-D200 leu2-D1*		(Sikorski and Hieter 1989)
YPH499 ADE2	*ade2::ADE2* (pRS402)	YPH499	
BY4741	*MAT***a** *his3Δ1 leu2Δ0 met15Δ0 ura3Δ0*		Invitrogen
Mnn9-mCherry	*ade2::ADE2* (pRS402) *MNN9-mCherry-natNT2*	YPH499	
ret1-1	*MAT***a** *ret1-1 ura3 leu2 his3 try1 suc2D9*	EGY101	(Letourneur et al. 1994)
sec21-1	*sec21-1 ura3*		
sec21-2	*sec21-2 ura3*		
	RET1-IAA17-kanMX	YPH499 ADE2	This study
Ret1-aid	*RET1-IAA17-kanMX ura3::pMK76*	YPH499 ADE2	This study
	RET1-IAA17-kanMX ura3::pMK76 MNN9-mCherry-natNT2	YPH499 ADE2	This study
	SEC21-IAA17-kanMX	YPH499 ADE2	This study
Sec21-aid	SEC21-IAA17-kanMX ura3::pMK76	YPH499 ADE2	This study
	SEC21-IAA17-kanMX ura3::pMK76 MNN9-mCherry-natNT2	YPH499 ADE2	This study
	RET1-IAA17-kanMX ura3::pMK76 MNN9-mCherry-natNT2 trp1::SEC71promoter-SEC71TMD-GFP-SEC71terminator	YPH499 ADE2	This study
	SEC21-IAA17-kanMX ura3::pMK76 MNN9-mCherry-natNT2 trp1::SEC71promoter-SEC71TMD-GFP-SEC71terminator	YPH499 ADE2	This study
cog5Δ	*cog5::kanMX6*	BY4741	Invitrogen
cog6Δ	*cog6::kanMX6*	BY4741	Invitrogen
cog7Δ	*cog7::kanMX6*	BY4741	Invitrogen
cog8Δ	*cog8::kanMX6*	BY4741	Invitrogen
cog5Δ	*cog5::kanMX6*	YPH499 ADE2	This study
cog6Δ	*cog6::kanMX6*	YPH499 ADE2	This study
cog7Δ	*cog7::kanMX6*	YPH499 ADE2	This study
cog8Δ	*cog8::kanMX6*	YPH499 ADE2	This study
CIT1-GFP	*CIT1-GFP-HIS3MX6*	BY4741	Invitrogen
SUC2-13Myc	*SUC2::SUC2-13Myc*	YPH499 ADE2	This study
COG1-GFP	*COG1-GFP-HIS3MX6*	BY4741	Invitrogen
COG3-GFP	*COG3-GFP-HIS3MX6*	BY4741	Invitrogen
COG5-GFP	*COG5-GFP-HIS3MX6*	BY4741	Invitrogen
COG6-GFP	*COG6-GFP-HIS3MX6*	BY4741	Invitrogen
	ura3::GAL1promoter-COG1-mCherry-FIS1	YPH499 ADE2	This study
	ura3::GAL1promoter-COG2-mCherry-FIS1	YPH499 ADE2	This study
	ura3::GAL1promoter-COG3-mCherry-FIS1	YPH499 ADE2	This study
	ura3::GAL1promoter-COG4-mCherry-FIS1	YPH499 ADE2	This study
	ura3::GAL1promoter-COG5-mCherry-FIS1	YPH499 ADE2	This study
	ura3::GAL1promoter-COG6-mCherry-FIS1	YPH499 ADE2	This study
	ura3::GAL1promoter-COG7-mCherry-FIS1	YPH499 ADE2	This study
	ura3::GAL1promoter-COG8-mCherry-FIS1	YPH499 ADE2	This study
	cog5::kanMX6 ura3::GAL1promoter-COG5-mCherry-FIS1	YPH499 ADE2	This study
	cog6::kanMX6 ura3::GAL1promoter-COG6-mCherry-FIS1	YPH499 ADE2	This study
	cog7::kanMX6 ura3::GAL1promoter-COG7-mCherry-FIS1	YPH499 ADE2	This study
	cog8::kanMX6 ura3::GAL1promoter-COG8-mCherry-FIS1	YPH499 ADE2	This study
	SUC2::SUC2-13Myc ura3::GAL1promoter-COG1-mCherry-FIS1	YPH499 ADE2	This study
	SUC2::SUC2-13Myc ura3::GAL1promoter-COG2-mCherry-FIS1	YPH499 ADE2	This study
	SUC2::SUC2-13Myc ura3::GAL1promoter-COG3-mCherry-FIS1	YPH499 ADE2	This study

SUC2::SUC2-13Myc ura3::GAL1promoter-COG4-mCherry-FIS1	YPH499 ADE2	This study
SUC2::SUC2-13Myc ura3::GAL1promoter-COG5-mCherry-FIS1	YPH499 ADE2	This study
SUC2::SUC2-13Myc ura3::GAL1promoter-COG6-mCherry-FIS1	YPH499 ADE2	This study
SUC2::SUC2-13Myc ura3::GAL1promoter-COG7-mCherry-FIS1	YPH499 ADE2	This study
SUC2::SUC2-13Myc ura3::GAL1promoter-COG8-mCherry-FIS1	YPH499 ADE2	This study

Table 2　Plasmids used this study

Plasmid name	Description	Source
pRS316-ADH1p-GNT1-GFP-CMK1t	*URA3, CEN*	This study
pRS316-ADH1p-SYS1-GFP-CMK1t	*URA3, CEN*	This study
pRS316-ADH1p-SEC7-GFP-TDH3p-mRFP-SED5	*URA3, CEN*	(Matsuura-Tokita et al. 2006)
pRS304-SEC71p-SEC71TMD-GFP-SEC71t	*TRP1*, integration	This study
pRS316-GFP-SED5	*URA3, CEN, TDH3* promoter	(Matsuura-Tokita et al. 2006)
pRS316-GFP-GOS1	*URA3, CEN, TDH3* promoter	(Matsuura-Tokita et al. 2006)
pRS316-SEC7-GFP	*URA3, CEN, ADH1* promoter	(Matsuura-Tokita et al. 2006)
pRS316-SEC7-mRFP	*URA3, CEN, ADH1* promoter	(Matsuura-Tokita et al. 2006)
pRS314-GNT1-GFP	*TRP1, CEN, ADH1* promoter	This study
pRS314-SYS1-GFP	*TRP1, CEN, ADH1* promoter	This study
pRS314-GFP-TLG1	*TRP1, CEN, ADH1* promoter	Y. Suda
pRS402	*ADE2*, integration	(Brachmann et al. 1998)
pFA6a-mCherry-natNT2	PCR template	(Kurokawa et al. 2014)
pMK43	PCR template, IAA17-kanMX	National BioResource Project (NBRP), Japan
pMK76	*URA3*, integration, *ADH1p-AtTIR1-9Myc*	National BioResource Project (NBRP), Japan
pYES2	*URA3, 2μ, GAL1* promoter	Invitrogen
pYES2-FIS1	*URA3, 2μ, GAL1* promoter	This study
pYES2-mCherry-FIS1	*URA3, 2μ, GAL1* promoter	This study
pYES2-COG1-mCherry-FIS1	*URA3, 2μ, GAL1* promoter	This study
pYES2-COG2-mCherry-FIS1	*URA3, 2μ, GAL1* promoter	This study
pYES2-COG3-mCherry-FIS1	*URA3, 2μ, GAL1* promoter	This study
pYES2-COG4-mCherry-FIS1	*URA3, 2μ, GAL1* promoter	This study
pYES2-COG5-mCherry-FIS1	*URA3, 2μ, GAL1* promoter	This study
pYES2-COG6-mCherry-FIS1	*URA3, 2μ, GAL1* promoter	This study
pYES2-COG7-mCherry-FIS1	*URA3, 2μ, GAL1* promoter	This study
pYES2-COG8-mCherry-FIS1	*URA3, 2μ, GAL1* promoter	This study
pRS306-GAL1pr-COG1-mCherry-FIS1-CYC1term	URA3, integration	This study
pRS306-GAL1pr-COG2-mCherry-FIS1-CYC1term	URA3, integration	This study
pRS306-GAL1pr-COG3-mCherry-FIS1-CYC1term	URA3, integration	This study
pRS306-GAL1pr-COG4-mCherry-FIS1-CYC1term	URA3, integration	This study
pRS306-GAL1pr-COG5-mCherry-FIS1-CYC1term	URA3, integration	This study
pRS306-GAL1pr-COG6-mCherry-FIS1-CYC1term	URA3, integration	This study
pRS306-GAL1pr-COG7-mCherry-FIS1-CYC1term	URA3, integration	This study
pRS306-GAL1pr-COG8-mCherry-FIS1-CYC1term	URA3, integration	This study
pYES2-COG1	*URA3, 2μ, GAL1* promoter	This study
pYES2-COG2	*URA3, 2μ, GAL1* promoter	This study
pYES2-COG3	*URA3, 2μ, GAL1* promoter	This study
pYES2-COG4	*URA3, 2μ, GAL1* promoter	This study
pYES2-COG5	*URA3, 2μ, GAL1* promoter	This study
pYES2-COG6	*URA3, 2μ, GAL1* promoter	This study
pYES2-COG7	*URA3, 2μ, GAL1* promoter	This study
pYES2-COG8	*URA3, 2μ, GAL1* promoter	This study
pRS304-SUC2-13Myc-ADH1term	*TRP1,* integration	This study

Table 3 Primers used this study

Name	Sequence 5´ to 3´
SacI-ADH1p-F	GATC GAGCTC TGCCATCTATTGAAGTAATAATAGG
ADH1p-NotI-R	GATC GCGGCCGC TGTATATGAGATAGTTGATTGTATGC
XhoI-CMK1t-F	GATC CTCGAG TTGCACAATTAGTTAACACA
CMK1t-SacI-KpnI-R	GATC GGTACC GAGCTC ATCGATGAGTGCCCAATTCA
SalI-GFP-F	GATC GTCGAC ATGGTGAGCAAGGGCGAGGA
GFP-XhoI-R	GATC CTCGAG TTATACAGCTCGTCCATGCCGAGAG
NotI-GNT1-F	GATC GCGGCCGC ATGAGGTTGATATCCAAAAG
GNT1w/oStop-SalI-R	GATC GTCGAC AACGAGGCAGATTTCCCTGG
XbaI-SYS1-F	GATC TCTAGA ATGGTTTCGATAAGAAGGTA
SYS1s/oStop-HindIII-R	GATC AAGCTT TATTTGGCTTTCTAAGTCTT
RET1-S3	AATTGCTATGATTTCTAAGATCGGTGCACCTGCATCCGGATTAAGAATACGT GTA CGTACGCTGCAGGTCGAC
RET1-S2	ATTTAGGTCGAGCAGAATACAATCCCGAGAAAATCAATAGGCAAAATAGCAT TTA ATCGATGAATTCGAGCTCG
SEC21-S3	TGGTAAAGGTGAAGACAGCTTATTATGCTCTGATCTGGTGAATGGTCTAATG CAG CGTACGCTGCAGGTCGAC
SEC21-S2	TTAATACTATTGATAACAAAAGAAGGGATTAACTGAAATAAAATTTCACAGCT TA ATCGATGAATTCGAGCTCG
KpnI-FIS1-F	GATCGGTACCATGACCAAAGTAGATTTTTGG
FIS1w/Stop-NotI-R	GATCGCGGCCGCTTACCTTCTCTTGTTTCTTA
BamHI-xFP in pYES2 InFu-Fwd	ATTAAGCTTGGTACCGGATCCATGGTGAGCAAGGGCGAGGA
xFP-BamHI in pYES2 InFu-Rev	ATCTACTTTGGTCATGGATCCCTTGTACAGCTCGTCCATGC
HindIII-COG2-F	GATCAAGCTTATGGACTTTTTGAATGATGA
COG2w/oStop-KpnI-R	GATCGGTACCTGCCGTTTTTATAATGGAGA
HindIII-COG3-F	GATCAAGCTTATGGCGAGAAGTAGAAAGAA
Cog3w/oStop-KpnI-R	GATCGGTACCTTTCGTTATGGTATCAATAT
HindIII-COG4-F	GATCAAGCTTATGGAAGGGCAAAAATCGAATG
COG4w/oStop-KpnI-R	GATCGGTACCCTGTGTTCTATCAATCTTCATATTTC
HindIII-COG5-F	GATCAAGCTTATGACAATAGCGCCAATGGC
COG5w/oStop-KpnI-R	GATCGGTACCCTTATTTAGAGAAATAGATAC
HindIII-COG1 in pYES2 InFu-Fwd	AGGGAATATTAAGCTTATGGATGAAGTCTTACCATT
COG1w/oStop-KpnI in pYES2-mCh-FIS1 InFu-Rev	CTCACCATGGATCCGGTACCCTGTTGCCTTAATTGAGTAA
HindIII-COG6 in pYES2 InFu-Fwd	AGGGAATATTAAGCTTATGGATTTCGTTGTAGACTA
COG6w/oStop-KpnI in pYES2-mCh-FIS1 InFu-Rev	CTCACCATGGATCCGGTACCGTGATCAATACCTATCAACA
HindIII-COG7 in pYES2 InFu-Fwd	AGGGAATATTAAGCTTATGGTAGAGTTGACAATTAC
COG7w/oStop-KpnI in pYES2-mCh-FIS1 InFu-Rev	CTCACCATGGATCCGGTACCTGATATCATACCATCGTCAA
HindIII-COG8 in pYES2 InFu-Fwd	AGGGAATATTAAGCTTATGGAGCTGATACTAAACAG
COG8w/oStop-KpnI in pYES2-mCh-FIS1 InFu-Rev	CTCACCATGGATCCGGTACCGGAGTATATATATTTAGAGG
NotI-COG1-F	GATC GCGGCCGC ATGGATGAAGTCTTACCATT
COG1/wStop-XhoI-R	GATC CTCGAG TTACTGTTGCCTTAATTGAG
COG2w/Stop-KpnI-R	GATC GGTACC CTATGCCGTTTTTATAATGG
NotI-COG3-F	GATC GCGGCCGC ATGGCGAGAAGTAGAAAGAA
COG3w/Stop-XhoI-R	GATC CTCGAG TTATTTCGTTATGGTATCAATATC
COG4w/Stop-XhoI-R	GATCCTCGAGTTACTGTGTTCTATCAATCTTCATATTTC
BamHI-COG5-F	GATC GGATCC ATGACAATAGCGCCAATGGC
COG5w/Stop-SalI-R	GATC GTCGAC TCACTTATTTAGAGAAATAG
BamHI-COG6-F	GATC GGATCC ATGGATTTCGTTGTAGACTATC
COG6w/Stop-SalI-R	GATC GTCGAC TCAGTGATCAATACCTATCAAC

BamHI-COG7-F	GATC GGATCC ATGGTAGAGTTGACAATTAC
COG7s/Stop-SalI-R	GATC GTCGAC GACGATGGTATGATATCATAA
BamHI-COG8-F	GATCGGATCCATGGAGCTGATACTAAACAG
COG8w/Stop-SalI-R	GATC GTCGAC CTAGGAGTATATATATTTAG
XhoI-Myc-F	GTCGACGGATCCCCGGGTTAATTAACGGTCTCGAGGAACAAAAGCTAATC
ADH1t-KpnI-R	GATCGGTACCCCGGTAGAGGTGTGGTCAAT
SacI-SUC2-F	GATCGAGCTCATGCTTTTGCAAGCTTTCCT
SUC2w/oStop-XhoI-R	GATCCTCGAGTTTTACTTCCCTTACTTGGAACTTG
SacII-GAL1p-F	GATC CCGCGG CGGATTAGAAGCCGCCGAGC
CYC1term-SalI-R	GATC GTCGAC GGCCGCAAATTAAAGCCTTC
CYC1t-SmaI-R	GATC CCCGGG GCAAATTAAAGCCTTCGAGC
COG1-Ctag-F	ACAATCTCTTGCAATTAGTCATCGATCAAATTACTCAATTAAGGCAACAG GGATCGAGCGCATCGGGTGC
COG1-S2	ATCATTATCAATAAGTTTGCGAGGCGGGTACCCTCCCTCGTGCTATTATA ATCGATGAATTCGAGCTCG
COG2-Ctag-F	CAAGCCTGCAAAACCTATCTTTGACATTAGTCTCCATTATAAAAACGGCA GGATCGAGCGCATCGGGTGC
COG2-S2	TAAAATACTTATATCAGTCCACAATTGAAGTATGGAAAGTTTTCTCCCAA ATCGATGAATTCGAGCTCG
COG3-Ctag-F	AAGAGGTGGCGGATCTTTTAAGAAATGGTGATATTGATACCATAACGAAA GGATCGAGCGCATCGGGTGC
COG3-S2	GATTTATGTATGCATGAAAATTATAGAAAAAGTTGAAATTACACATAAGT ATCGATGAATTCGAGCTCG
COG4-Ctag-F	ACTCTCAGGAAAGAATTAAAGCTAGAAATATGAAGATTGATAGAACACAG GGATCGAGCGCATCGGGTGC
COG4-S2	GCGTTTATATGAAACTACTTAGTATTCAGCTCGTAAAGCTTATGTTATAT ATCGATGAATTCGAGCTCG
COG5-Ctag-F	AAAGCTACTTGGATGTAATGCTAAACTCAGTATCTATTTCTCTAAATAAG GGATCGAGCGCATCGGGTGC
COG5-S2	CTTTAGATTCATCCTATTTCATCAACATTCTTAATTTTATGTAAACTGTC ATCGATGAATTCGAGCTCG
COG6-Ctag-F	TTTTAAATTTTTCCACTGATGAATTTGACATGTTGATAGGTATTGATCAC GGATCGAGCGCATCGGGTGC
COG6-S2	GGGCAAGATGCGTCTTTGTGAGACGATTTTAAACAGAAGTTGTTCATCTC ATCGATGAATTCGAGCTCG
COG7-Ctag-F	AAGCACAAAGTTATTTATCAACCAAGAATATTGACGATGGTATGATATCA GGATCGAGCGCATCGGGTGC
COG7-S2	ATGCTATAAATTTCTTTTGTTAATTGCAAATTTTTTGTTTTTATCACCGA ATCGATGAATTCGAGCTCG
COG8-Ctag-F	CCCGGGCAATTGACAAGAGAGCAGAACTGGCCTCTAAATATATATACTCC GGATCGAGCGCATCGGGTGC
COG8-S2	AAATTTCGGACGATCGTCATTTTGAAAATACATAGTGAGCCAATATTATA ATCGATGAATTCGAGCTCG
COG6upATG100b-F	TTCATACAAAATATACATCT
COG6downStop100b-R	ATAGATACCCGCCGCATACC
COG8upATG100b-F	CAATGTCTAAAAATATAGCG
COG8downStop100b-R	CATTCTCGTATTGTTGTTTC
COG5upATG200b-F	TTCTTATATTTAAGGGAACC
COG5downStop200b-R	AGGACAGAATGACCACGTAA
COG7upATG200b-F	ATGGGGAGGTGCTTGAAGTT
COG7downStop200b-R	AAGATGTGTGTAATAGTTAT
NotI-xFP-F	GATC GCGGCCGC ATGGTGAGCAAGGGCGAGGA
xFPw/oStop-XbaI-R	GATC TCTAGA CTTGTACAGCTCGTCCATGC
BamHI-TLG1-F	GATC GGATCC ATGAACAACAGTGAAGATCC
TLG1w/Stop-EcoRI-R	GATC GAATTC TCAAGCAATGAATGCCAAAA

Reference

Achstetter, T., A. Franzusoff, C. Field and R. Schekman (1988). "SEC7 encodes an unusual, high molecular weight protein required for membrane traffic from the yeast Golgi apparatus." J Biol Chem **263**(24): 11711-11717.

Behnia, R., B. Panic, J. R. Whyte and S. Munro (2004). "Targeting of the Arf-like GTPase Arl3p to the Golgi requires N-terminal acetylation and the membrane protein Sys1p." Nat Cell Biol **6**(5): 405-413.

Bhave, M., E. Papanikou, P. Iyer, K. Pandya, B. K. Jain, A. Ganguly, C. Sharma, K. Pawar, J. Austin, 2nd, K. J. Day, O. W. Rossanese, B. S. Glick and D. Bhattacharyya (2014). "Golgi enlargement in Arf-depleted yeast cells is due to altered dynamics of cisternal maturation." J Cell Sci **127**(Pt 1): 250-257.

Bonfanti, L., A. A. Mironov, Jr., J. A. Martinez-Menarguez, O. Martella, A. Fusella, M. Baldassarre, R. Buccione, H. J. Geuze, A. A. Mironov and A. Luini (1998). "Procollagen traverses the Golgi stack without leaving the lumen of cisternae: evidence for cisternal maturation." Cell **95**(7): 993-1003.

Brachmann, C. B., A. Davies, G. J. Cost, E. Caputo, J. Li, P. Hieter and J. D. Boeke (1998). "Designer deletion strains derived from Saccharomyces cerevisiae S288C: a useful set of strains and plasmids for PCR-mediated gene disruption and other applications." Yeast **14**(2): 115-132.

Bruinsma, P., R. G. Spelbrink and S. F. Nothwehr (2004). "Retrograde transport of the mannosyltransferase Och1p to the early Golgi requires a component of the COG transport complex." J Biol Chem **279**(38): 39814-39823.

Cosson, P., M. Amherdt, J. E. Rothman and L. Orci (2002). "A resident Golgi protein is excluded from peri-Golgi vesicles in NRK cells." Proc Natl Acad Sci U S A **99**(20): 12831-12834.

Daboussi, L., G. Costaguta and G. S. Payne (2012). "Phosphoinositide-mediated clathrin adaptor progression at the trans-Golgi network." Nat Cell Biol **14**(3): 239-248.

Emr, S., B. S. Glick, A. D. Linstedt, J. Lippincott-Schwartz, A. Luini, V. Malhotra, B. J. Marsh, A. Nakano, S. R. Pfeffer, C. Rabouille, J. E. Rothman, G. Warren and F. T. Wieland (2009). "Journeys through the Golgi--taking stock in a new era." J Cell Biol **187**(4): 449-453.

Fotso, P., Y. Koryakina, O. Pavliv, A. B. Tsiomenko and V. V. Lupashin (2005). "Cog1p plays a central role in the organization of the yeast conserved oligomeric Golgi complex." J Biol Chem **280**(30): 27613-27623.

Freeze, H. H. and B. G. Ng (2011). "Golgi glycosylation and human inherited diseases." Cold Spring Harb Perspect Biol **3**(9): a005371.

Fridy, P. C., Y. Li, S. Keegan, M. K. Thompson, I. Nudelman, J. F. Scheid, M. Oeffinger, M. C. Nussenzweig, D. Fenyo, B. T. Chait and M. P. Rout (2014). "A robust pipeline for rapid production of versatile nanobody repertoires." Nat Methods **11**(12): 1253-1260.

Gabriely, G., R. Kama and J. E. Gerst (2007). "Involvement of specific COPI subunits in protein sorting from the late endosome to the vacuole in yeast." Mol Cell Biol **27**(2): 526-540.

Glick, B. S. and A. Luini (2011). "Models for Golgi traffic: a critical assessment." Cold Spring Harb Perspect Biol **3**(11): a005215.

Glick, B. S. and A. Nakano (2009). "Membrane traffic within the Golgi apparatus." Annu Rev Cell Dev Biol **25**: 113-132.

Ha, J. Y., H. T. Chou, D. Ungar, C. K. Yip, T. Walz and F. M. Hughson (2016). "Molecular architecture of the complete COG tethering complex." Nat Struct Mol Biol **23**(8): 758-760.

Hardwick, K. G. and H. R. Pelham (1992). "SED5 encodes a 39-kD integral membrane protein required for vesicular transport between the ER and the Golgi complex." J Cell Biol **119**(3): 513-521.

Hirata, R., C. Nihei and A. Nakano (2013). "Isoform-selective oligomer formation of Saccharomyces cerevisiae p24 family proteins." J Biol Chem **288**(52): 37057-37070.

Jungmann, J. and S. Munro (1998). "Multi-protein complexes in the cis Golgi of Saccharomyces cerevisiae with alpha-1,6-mannosyltransferase activity." EMBO J **17**(2): 423-434.

Kurokawa, K., M. Ishii, Y. Suda, A. Ichihara and A. Nakano (2013). "Live cell visualization of Golgi membrane dynamics by super-resolution confocal live imaging microscopy." Methods in cell biology **118**: 235-242.

Kurokawa, K., M. Ishii, Y. Suda, A. Ichihara and A. Nakano (2013). "Live cell visualization of Golgi membrane dynamics by super-resolution confocal live imaging microscopy." Methods Cell Biol **118**: 235-242.

Kurokawa, K., M. Okamoto and A. Nakano (2014). "Contact of cis-Golgi with ER exit sites executes cargo capture and delivery from the ER." Nat Commun **5**: 3653.

Laufman, O., W. Hong and S. Lev (2013). "The COG complex interacts with multiple Golgi SNAREs and enhances fusogenic assembly of SNARE complexes." J Cell Sci **126**(Pt 6): 1506-1516.

Lee, C. and J. Goldberg (2010). "Structure of coatomer cage proteins and the relationship among COPI, COPII, and clathrin vesicle coats." Cell **142**(1): 123-132.

Lees, J. A., C. K. Yip, T. Walz and F. M. Hughson (2010). "Molecular organization of the COG vesicle tethering complex." Nat Struct Mol Biol **17**(11): 1292-1297.

Letourneur, F., E. C. Gaynor, S. Hennecke, C. Demolliere, R. Duden, S. D. Emr, H. Riezman and P. Cosson (1994). "Coatomer is essential for retrieval of dilysine-tagged proteins to the endoplasmic reticulum." Cell **79**(7): 1199-1207.

Longtine, M. S., A. McKenzie, 3rd, D. J. Demarini, N. G. Shah, A. Wach, A. Brachat, P. Philippsen and J. R. Pringle (1998). "Additional modules for versatile and economical PCR-based gene deletion and

modification in Saccharomyces cerevisiae." Yeast **14**(10): 953-961.

Losev, E., C. A. Reinke, J. Jellen, D. E. Strongin, B. J. Bevis and B. S. Glick (2006). "Golgi maturation visualized in living yeast." Nature **441**(7096): 1002-1006.

Luini, A. (2011). "A brief history of the cisternal progression-maturation model." Cell Logist **1**(1): 6-11.

Luo, G., J. Zhang and W. Guo (2014). "The role of Sec3p in secretory vesicle targeting and exocyst complex assembly." Mol Biol Cell **25**(23): 3813-3822.

Malsam, J., A. Satoh, L. Pelletier and G. Warren (2005). "Golgin tethers define subpopulations of COPI vesicles." Science **307**(5712): 1095-1098.

Martinez-Menarguez, J. A., R. Prekeris, V. M. Oorschot, R. Scheller, J. W. Slot, H. J. Geuze and J. Klumperman (2001). "Peri-Golgi vesicles contain retrograde but not anterograde proteins consistent with the cisternal progression model of intra-Golgi transport." J Cell Biol **155**(7): 1213-1224.

Matsuura-Tokita, K., M. Takeuchi, A. Ichihara, K. Mikuriya and A. Nakano (2006). "Live imaging of yeast Golgi cisternal maturation." Nature **441**(7096): 1007-1010.

Mowbrey, K. and J. B. Dacks (2009). "Evolution and diversity of the Golgi body." FEBS Lett **583**(23): 3738-3745.

Mozdy, A. D., J. M. McCaffery and J. M. Shaw (2000). "Dnm1p GTPase-mediated mitochondrial fission is a multi-step process requiring the novel integral membrane component Fis1p." J Cell Biol **151**(2): 367-380.

Munro, S. (2011). "The golgin coiled-coil proteins of the Golgi apparatus." Cold Spring Harb Perspect Biol **3**(6).

Nakano, A. and A. Luini (2010). "Passage through the Golgi." Curr Opin Cell Biol **22**(4): 471-478.

Nishimura, K., T. Fukagawa, H. Takisawa, T. Kakimoto and M. Kanemaki (2009). "An auxin-based degron system for the rapid depletion of proteins in nonplant cells." Nature methods **6**(12): 917-922.

Orci, L., M. Ravazzola, A. Volchuk, T. Engel, M. Gmachl, M. Amherdt, A. Perrelet, T. H. Sollner and J. E. Rothman (2000). "Anterograde flow of cargo across the golgi stack potentially mediated via bidirectional "percolating" COPI vesicles." Proc Natl Acad Sci U S A **97**(19): 10400-10405.

Orci, L., M. Stamnes, M. Ravazzola, M. Amherdt, A. Perrelet, T. H. Sollner and J. E. Rothman (1997). "Bidirectional transport by distinct populations of COPI-coated vesicles." Cell **90**(2): 335-349.

Ostermann, J., L. Orci, K. Tani, M. Amherdt, M. Ravazzola, Z. Elazar and J. E. Rothman (1993). "Stepwise assembly of functionally active transport vesicles." Cell **75**(5): 1015-1025.

Papanikou, E., K. J. Day, J. Austin and B. S. Glick (2015). "COPI selectively drives maturation of the early Golgi." Elife **4**.

Pellett, P. A., F. Dietrich, J. Bewersdorf, J. E. Rothman and G. Lavieu (2013). "Inter-Golgi transport

mediated by COPI-containing vesicles carrying small cargoes." Elife **2**: e01296.

Rabouille, C. and J. Klumperman (2005). "Opinion: The maturing role of COPI vesicles in intra-Golgi transport." Nat Rev Mol Cell Biol **6**(10): 812-817.

Ram, R. J., B. Li and C. A. Kaiser (2002). "Identification of Sec36p, Sec37p, and Sec38p: components of yeast complex that contains Sec34p and Sec35p." Mol Biol Cell **13**(5): 1484-1500.

Rivera-Molina, F. E. and P. J. Novick (2009). "A Rab GAP cascade defines the boundary between two Rab GTPases on the secretory pathway." Proc Natl Acad Sci U S A **106**(34): 14408-14413.

Rizzo, R., S. Parashuraman, P. Mirabelli, C. Puri, J. Lucocq and A. Luini (2013). "The dynamics of engineered resident proteins in the mammalian Golgi complex relies on cisternal maturation." J Cell Biol **201**(7): 1027-1036.

Rothman, J. E. and F. T. Wieland (1996). "Protein sorting by transport vesicles." Science **272**(5259): 227-234.

Sato, K. and A. Nakano (2003). "Oligomerization of a cargo receptor directs protein sorting into COPII-coated transport vesicles." Mol Biol Cell **14**(7): 3055-3063.

Sato, K., M. Sato and A. Nakano (2001). "Rer1p, a retrieval receptor for endoplasmic reticulum membrane proteins, is dynamically localized to the Golgi apparatus by coatomer." J Cell Biol **152**(5): 935-944.

Sato, K., M. Sato and A. Nakano (2003). "Rer1p, a retrieval receptor for ER membrane proteins, recognizes transmembrane domains in multiple modes." Mol Biol Cell **14**(9): 3605-3616.

Schindelin, J., I. Arganda-Carreras, E. Frise, V. Kaynig, M. Longair, T. Pietzsch, S. Preibisch, C. Rueden, S. Saalfeld, B. Schmid, J. Y. Tinevez, D. J. White, V. Hartenstein, K. Eliceiri, P. Tomancak and A. Cardona (2012). "Fiji: an open-source platform for biological-image analysis." Nat Methods **9**(7): 676-682.

Schmitz, K. R., J. Liu, S. Li, T. G. Setty, C. S. Wood, C. G. Burd and K. M. Ferguson (2008). "Golgi localization of glycosyltransferases requires a Vps74p oligomer." Dev Cell **14**(4): 523-534.

Sengupta, D., S. Truschel, C. Bachert and A. D. Linstedt (2009). "Organelle tethering by a homotypic PDZ interaction underlies formation of the Golgi membrane network." J Cell Biol **186**(1): 41-55.

Serafini, T., L. Orci, M. Amherdt, M. Brunner, R. A. Kahn and J. E. Rothman (1991). "ADP-ribosylation factor is a subunit of the coat of Golgi-derived COP-coated vesicles: a novel role for a GTP-binding protein." Cell **67**(2): 239-253.

Shestakova, A., E. Suvorova, O. Pavliv, G. Khaidakova and V. Lupashin (2007). "Interaction of the conserved oligomeric Golgi complex with t-SNARE Syntaxin5a/Sed5 enhances intra-Golgi SNARE complex stability." J Cell Biol **179**(6): 1179-1192.

Sikorski, R. S. and P. Hieter (1989). "A system of shuttle vectors and yeast host strains designed for efficient manipulation of DNA in Saccharomyces cerevisiae." Genetics **122**(1): 19-27.

Suda, Y., K. Kurokawa, R. Hirata and A. Nakano (2013). "Rab GAP cascade regulates dynamics of Ypt6 in the Golgi traffic." Proc Natl Acad Sci U S A **110**(47): 18976-18981.

Suvorova, E. S., R. Duden and V. V. Lupashin (2002). "The Sec34/Sec35p complex, a Ypt1p effector required for retrograde intra-Golgi trafficking, interacts with Golgi SNAREs and COPI vesicle coat proteins." J Cell Biol **157**(4): 631-643.

Tu, L., W. C. Tai, L. Chen and D. K. Banfield (2008). "Signal-mediated dynamic retention of glycosyltransferases in the Golgi." Science **321**(5887): 404-407.

VanRheenen, S. M., X. Cao, V. V. Lupashin, C. Barlowe and M. G. Waters (1998). "Sec35p, a novel peripheral membrane protein, is required for ER to Golgi vesicle docking." J Cell Biol **141**(5): 1107-1119.

VanRheenen, S. M., X. Cao, S. K. Sapperstein, E. C. Chiang, V. V. Lupashin, C. Barlowe and M. G. Waters (1999). "Sec34p, a protein required for vesicle tethering to the yeast Golgi apparatus, is in a complex with Sec35p." J Cell Biol **147**(4): 729-742.

Whyte, J. R. and S. Munro (2001). "The Sec34/35 Golgi transport complex is related to the exocyst, defining a family of complexes involved in multiple steps of membrane traffic." Dev Cell **1**(4): 527-537.

Willett, R., J. B. Blackburn, L. Climer, I. Pokrovskaya, T. Kudlyk, W. Wang and V. Lupashin (2016). "COG lobe B sub-complex engages v-SNARE GS15 and functions via regulated interaction with lobe A sub-complex." Sci Rep **6**: 29139.

Willett, R., T. Kudlyk, I. Pokrovskaya, R. Schonherr, D. Ungar, R. Duden and V. Lupashin (2013). "COG complexes form spatial landmarks for distinct SNARE complexes." Nat Commun **4**: 1553.

Wong, M. and S. Munro (2014). "Membrane trafficking. The specificity of vesicle traffic to the Golgi is encoded in the golgin coiled-coil proteins." Science **346**(6209): 1256898.

Wood, C. S., C. S. Hung, Y. S. Huoh, C. J. Mousley, C. J. Stefan, V. Bankaitis, K. M. Ferguson and C. G. Burd (2012). "Local control of phosphatidylinositol 4-phosphate signaling in the Golgi apparatus by Vps74 and Sac1 phosphoinositide phosphatase." Mol Biol Cell **23**(13): 2527-2536.

Wuestehube, L. J., R. Duden, A. Eun, S. Hamamoto, P. Korn, R. Ram and R. Schekman (1996). "New mutants of Saccharomyces cerevisiae affected in the transport of proteins from the endoplasmic reticulum to the Golgi complex." Genetics **142**(2): 393-406.

Yahara, N., T. Ueda, K. Sato and A. Nakano (2001). "Multiple roles of Arf1 GTPase in the yeast exocytic and endocytic pathways." Mol Biol Cell **12**(1): 221-238.

Yang, J. S., C. Valente, R. S. Polishchuk, G. Turacchio, E. Layre, D. B. Moody, C. C. Leslie, M. H. Gelb,

W. J. Brown, D. Corda, A. Luini and V. W. Hsu (2011). "COPI acts in both vesicular and tubular transport." Nat Cell Biol **13**(8): 996-1003.

Yoko-o, T., C. A. Wiggins, J. Stolz, S. Y. Peak-Chew and S. Munro (2003). "An N-acetylglucosaminyltransferase of the Golgi apparatus of the yeast Saccharomyces cerevisiae that can modify N-linked glycans." Glycobiology **13**(8): 581-589.

The major part of the Chapter 1 has been published in Journal of Cell Science (The Company of Biologists Ltd) as an article entitled “COPI is essential for Golgi cisternal maturation and dynamics” by Midori Ishii, Yasuyuki Suda, Kazuo Kurokawa, and Akihiko Nakano (volume 129, issue 17, pages3251-3261 doi:10.1242/jcs.193367, http://jcs.biologists.org/content/129/17/3251).